universität wien

MASTERARBEIT / MASTER'S THESIS

Titel der Masterarbeit / Title of the Master's Thesis

„Investigation of a putative Toxin-Antitoxin system of the archaeal virus ΦCh1"

verfasst von / submitted by

Matthias Schmal BSc

angestrebter akademischer Grad / in partial fulfilment of the requirements for the degree of

Master of Science (MSc)

Wien, 2018 / Vienna 2018

Studienkennzahl lt. Studienblatt / degree programme code as it appears on the student record sheet:	A 066 830
Studienrichtung lt. Studienblatt / degree programme as it appears on the student record sheet:	Master Molecular Microbiology, Microbial Ecology and Immunology
Betreut von / Supervisor:	Ao. Univ.- Prof. Dipl.- Biol. Dr. Angela Witte

Acknoledgements

Hereby I want to thank my supervisor Ao. Univ.- Prof. Dipl.- Biol. Dr. Angela Witte for the opportunity to work in her laboratory and the immense support throughout my work there. Even the most trivial questions never met deaf ears and and her will always to help kept me going in the hardest times.

Big warm thanks also goes to my colleagues and friends Mikaela, Jana, Richard, Dina and Seyda for providing me assisting support or friendship when needed.

Additionally I want to express my gratitude towards my mother, brother and uncle. They are the reason why I can write this thesis. Thank you very much!

Abstract

The temperate virus ΦCh1 infects the haloalkaliphilic archeon *Natrialba magadii*. The open reading frame 44 (ORF44) has a PilT N terminal domain (PIN domain) according to Pfam analysis. ORF44 forms together with ORF43 an operon as they are co-transcribed and co-translated. This information lead to the hypothesis that the operon ORF43/44 is a toxin-antitoxin system (TA-system) belonging to the VapBC family of type II TA-systems. The VapBC TA-system consists of the stable toxin VapC, which exhibits RNase activity and the labile antitoxin VapB, which is able to neutralize the toxicty of its cognate toxin. These TA-operons are often autoregulated by either the antitoxin or the TA-complex.

Previous investigation showed that the gene product of ORF44 (gp44) has an impact on the expression of $ORF34_{52}$, which encodes the tailfibre protein and ORF94, which encodes a methyltransferase. In order to further characterize the putative toxin ORF44, a new target of gp44 was identified: ORF22. It was shown that gp22 is part of the viral capsid of ΦCh1 and the expression of ORF44 leads to an truncated gp22. This supports the hypothesis that ORF44 encodes for a RNase.

The autoregulatory function of the putative antitoxin gp43 was also matter of investigation. This experiment was planned to be done in an environment, which lacks the viral background, however the control for this experiment was infected. Nonetheless, it is shown that the promoter of the operon ORF43/44 is constitutively active. This backs up the theory that the operon ORF43/44 is a TA-system.

Table of contents

1 Introduction

1.1 *Archaea*

1.1.1 Phylogeny of *Archaea*

All living organisms can be divided in three major kingdoms: *Eukarya*, *Bacteria*, and *Archaea* (WOESE & FOX, 1977). In 1990, based on 16S rRNA sequence comparison, the two main phyla of *Crenarchaeota* and *Euryarchaeota* were proposed (WOESE *et al*., 1990). Due to limited cultivation possibilities of *Archaea*, their phylogeny stayed unaltered for many years. In the past twenty years, improvements of DNA sequencing technologies and culture-independent approaches led to an enormous increase of genomic data. With this data it is possible to understand the diversity of *Archaea* in a holistic way. A schematic representation of our current understanding of the relationships between *Eukarya*, *Bacteria*, and *Archaea* is shown in Figure 1. In this tree of life *Eukarya* (red) are a branch within the group of *Archaea*. This hypothesis was proposed in 2011 and suggests a two-domain tree of life (GUY & ETTEMA, 2011). *Bacteria* are shown in purple and *Archaea* in blue and green. '*Aigararchaeota'* and '*Korarchaeota'* are still proposed phyla and thus in apostrophes. Also the *DPANN* superphylum is under debate to be monophyletic (EME *et al*., 2017).

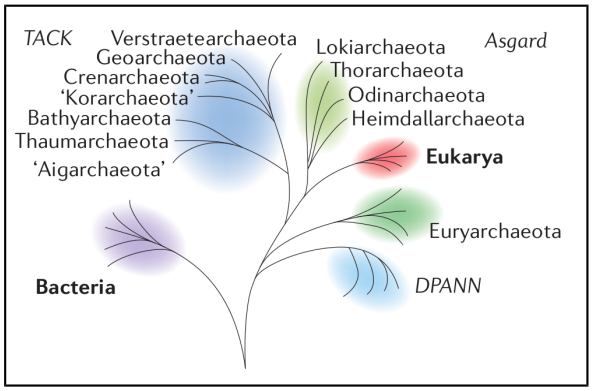

Figure 1: The tree of life. A schematic representation of our current understanding of the relationships between Eukarya (red), Archaea (blue and green) and Bacteria purple). Adapted from Eme *et al*, 2017.

1.1.2 Characteristics of *Archaea*

Even though *Archaea* belong to the kingdom of prokaryotes, they are clearly distinguishable from *Bacteria*. In addition they share some features with *Eukarya*, which are listed in Table 1 (CAVICCHIOLI, 2011). Some traits are unique to *Archaea*, like their membranes and ability for methanogenesis. However, the cell envelope is the most outstanding characteristic of *Archaea*.

Table 1: Shared traits of *Bacteria*, *Archaea* and *Eukarya*

Trait	*Bacteria*	*Archaea*	*Eukarya*
Carbon linkage of lipids	Ester	Ether	Ester
Phosphate backbone of lipids	Glycerol-3-phosphate	Glycerol-1-phosphate	Glycerol-3-phosphate
Metabolism	Bacterial	Bacterial-like	Eukaryotic-like
Core transcription apparatus	Bacterial	Eukaryotic-like	Eukaryotic
Translation elongation factors	Bacterial	Eukaryotic-like	Eukaryotic
Nucleus	No	No	Yes
Organelles	No	No	Yes
Methanogenesis	No	Yes	No
Genome organization	Bacterial	Bacterial	Eukaryotic

*The occurrence of a trait is for the majority of cases (not necessarily absolute) – for example, *haloarchaea* often possess organelles in the form of gas vesicles, however most *Archaea* posses no organelles (OREN, 2012).

1.1.2.1 Membranes of *Archaea*

Membranes of *Archaea* are unique in three ways: first, the hydrophobic core consits of isoprenoid structures in contrast to aliphatic acids of *Bacteria* and *Eukarya* (see Figure 2; compare **a** to **b** and **c**). Together with the ether-linkage of the isoprenoid-chain of glycerol,

the lipids are suited to best the harsh conditions in which *Archaea* are able to thrive, like high temperature or high salt concentrations (DE ROSA & GAMBACORTA, 1988). Exclusively unique to *Archaea* is the glycerol-1-phosphate (ALBERS & MEYER, 2011). The membranes of *Archaea* consist of either a lipid bilayer (see Figure 2**c**) or a tetraehter, forming a lipid monolayer (see Figure 2**b**).

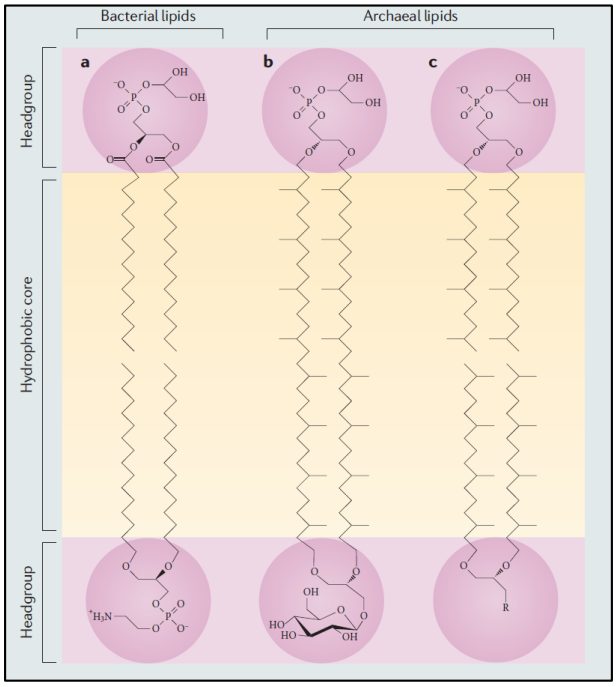

Figure 2: Differences of the hydrophobic core of membranes. a) Glycerol-3-phosphate is linked with ester bounds to aliphatic fatty acids; b) Two Glycerol-1-phosphate form a tetraether lipid leading to a monolayer; c) The membrane consists of a diether bilayer linked to Glycerol-1-phosphate. Adapted from Albers *et al*, 2011.

1.1.2.2 Surface-layer proteins on the cell envelope

Almost all *Archaea* have proteins or cell envelope polymers on the cell surface. The most widespread are the so called surface-layer (S-layer) proteins. These S-layer proteins differ in molecular weight from 40 to 200 kDa and in many cases are associated with the cytoplasmic membrane (ALBERS & MEYER, 2011). Additionally S-layer proteins are often glycosylated either *N*-linked or *O*-linked (see Fig. 3). In Figure 3 S-layer proteins of *Halobacteria, Sulfolobales, Thermusproteus* spp. and *Staphylothermus marinus* are shown (BAUMEISTER *et al*., 1989; PETERS *et al*., 1995). These proteins are able to intrinsically form two-dimensional crystalline arrays in an oblique, square or hexagonal symmetry (ALBERS & MEYER, 2011). The S-layer structure, depending on the symmetry, contains

two or more repeating pores. These pores have a diameter of 2-8 nm and can cover up to 70 % of the surface (ALBERS & MEYER, 2011).

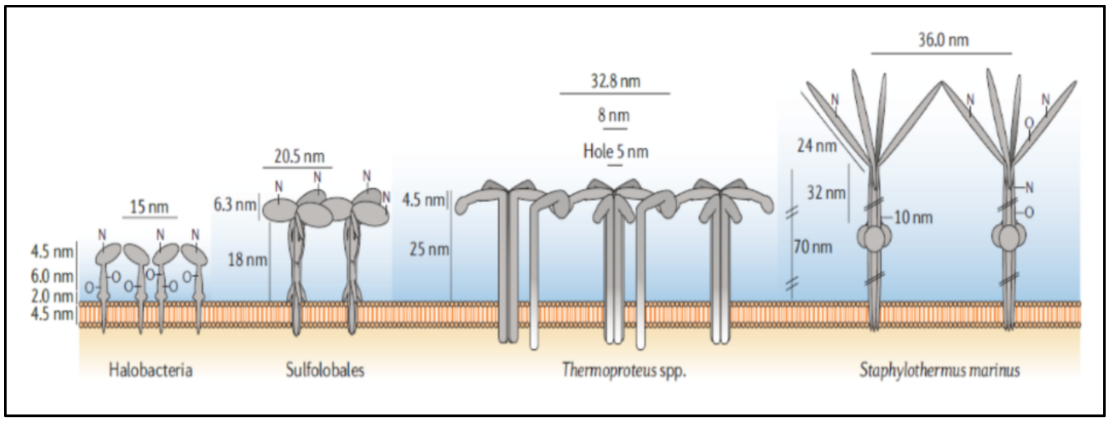

Figure 3: Side view of S-layer proteins of different Archaea. From left: Halobacteria, Sulfolobales, Thermusproteus spp. and Staphylothermus marinus. N, N-linked glycosylation; O, O-linked glycosylation. Adapted from Albers *et al*., 2011.

1.1.3 Haloalkaliphilic *Archaea*

Archaea are well known for their ability to thrive in extreme environments. They survive in temperatures ranging from 0°C, *Methanogenium frigidum* (FRANZMANN *et al*., 1997), to 122°C, *Methanopyrus kandleri* (TAKAI *et al*., 2008) and pH from 0, *Picrophilus oshimae* (SCHLEPER *et al*., 1995), to 11.0, *Natrialba magadii* (former *Natronobacterium magadii*) (TINDALL *et al*., 1984). Many *Archaea* can live in 'double-extreme' environments. Examples are thermoacidophiles, which prefer both high temperatures and low pH, or haloalkaliphiles, which prefer high concentration of salt and high pH. Haloalkaliphilic *Archaea* are only found within the phylum of *Euryarchaeota*.

1.1.3.1 Adaptations to high salinity

Halophilic organisms have to face two major challenges living in high salt surroundings: first high osmotic pressure and second low water activity. To counteract loss of water by osmosis, halophiles accumulate either organic or inorganic compounds within the cell

(GRANT, 2004). Therefore proteins must have adaptations to be soluble in low water activity environments. Halophilic proteins contain a huge excess of acidic amino acids over basic ones. Additionally the number of hydrophobic amino acids is low (MADERN *et al*., 1995).

1.1.3.2 Adaptations to high pH

Even though alkaliphiles can thrive in environments up to pH 11.4 (STURR *et al*., 1994), they have near-neutral pH within the cells to maintain protein function (COOK *et al*., 1996; GUFFANTI & HICKS, 1991; STURR *et al*., 1994). Two mechanisms help to survive these harsh conditions: first they keep their cell envelope negatively charged to trap protons for aerobic respiration (HAINES & DENCHER, 2002; TENCHOV *et al*., 2006) and second they have various numbers of Na^+/H^+-antiporters which pump Na^+ out and H^+ into the cells (HUNTE *et al*., 2005; ITO *et al*., 1997; KITADA *et al*., 1994; MESBAH *et al*., 2009).

1.1.4 *Natrialba magadii*

Natrialba magadii is a haloalkaliphilic archaeon and belongs to the order of *Halobacteriales* within the phylum of *Euryarchaeota*. It was first isolated and described in 1984 as *Natronobacterium magadii* and formed together with *Natronobacterium pharaonis* and *Natronobacterium gregoryi* the new genus *Natronobacterium* (TINDALL *et al*., 1984). In 1997 the 16S rRNA of *N. magadii* was compared to those of three other species of the genus of *Natronobacterium* and *N. magadii* was reclassified into the genus of *Natrialba* (KAMEKURA *et al*., 1997). The natural habitat of *N. magadii* is Lake Magadi in Kenya, which is a soda lake. These aquatic ecosystems are characterized by pH values of 9-12 and salinity up to saturation. *N. magadii* is chemoorganotrophic, obligately aerobic and alkaliphilic. It grows proteolytically, is rod-shaped and motility through a polar flagella can

be observed (TINDALL *et al*., 1984). Under laboratory conditions *N. magadii* needs rich medium containing 3.5-4 M NaCl and pH of 9-9.5 for optimal growth (TINDALL *et al*., 1984). The generation time is roughly 9 hours.

Genetic manipulations are possible in *N. magadii* after adapting a polyethylene glycol-based method for transformations of *Halobacterium salinarum* (former *Halobacterium halobium*) (CLINE & FORD DOOLITTLE, 1987; MAYRHOFER-IRO *et al*., 2013). Additionally two different vectors with different selection markers are available for *N. magadii*: pRo-5 and pNB102 (MAYRHOFER-IRO *et al*., 2013; ZHOU *et al*., 2004). Both have origins of replication for *Escherichia coli* as well as for halophilic *Archaea* and an ampicillin resistance cassette, thus making it possible to do all prior genetic manipulations in *E. coli*.

1.2 Archaeal viruses

Viruses are known to infect prokaryotes as well es *Eukarya*. The first archaeal virus was found in *H. salinarum* (TORSVIK & DUNDAS, 1974). Soon afterwards archaeal viruses were found in every ecosystem on earth, including thermal, extremely acidic and basic as well as hypersaline environments (BREITBART *et al*., 2004; MARTIN *et al*., 1984; OREN *et al*., 1997; WITTE *et al*., 1997). Culture independent methods also led to an enormous increase of genomic data of viruses and especially the archaeal ones. Yet, in most cases it is impossible to classify the viruses and moreover the hosts remain unknown.

Enumerate viruses in aquatic environments proofed to be difficult. However, estimations state that viruses may be the most abundant biological entities in aquatic ecosystems (WOMMACK & COLWELL, 2000). Together with the fact that viral predation is the primary cause for mortality in microbial communities, viruses play a substantial role in global geochemistry. Within the top 50 cm of marine sediments about 0.3-0.5 gigatonnes of

carbon are released each year mediated through virus-induced lysis of *Archaea* (DANOVARO *et al*., 2016).

1.2.1 Diverse morphology of archaeal viruses

The morphology of archaeal viruses is very diverse. Many of them have shapes that resemble those of bacterial phages and eukaryotic viruses, like classic head-tail or tailless icosahedral viruses. Head-tail viruses belong to the order of *Caudovirales*, which consists of three families: *Siphoviridae*, *Myoviridae* and *Podoviridae*. Tailless archaeal viruses belong to the families *Sphaerolipoviridae* and *Turriviridae* (PRANGISHVILI *et al*., 2017). However, viruses that infect hyperthermophilic *Crenarchaeota* have a broad range of unique morphologies. Their shapes vary from bottle-shaped *Ampullaviridae* (HÄRING, RACHEL, *et al*., 2005), lemon-shaped *Bicaudaviridae (*HÄRING, VESTERGAARD, *et al*., 2005; HOCHSTEIN *et al*., 2016), to coil-shaped *Spiraviridae* (MOCHIZUKI *et al*., 2012), droplet-shaped *Guttaviridae* (ARNOLD *et al*., 2000), filamentous *Lipothrixviridae* (BETTSTETTER *et al*., 2003) and rod-shaped *Rudiviridae* (PRANGISHVILI *et al*., 1999).

1.2.2 The haloalkaliphilic virus ΦCh1

The virus ΦCh1 was discovered upon spontaneous lysis of cultures of *N. magadii* when they reached the stationary growth phase (WITTE *et al*., 1997). It is the first described virus of haloalkaliphilic organisms and up to today *N. magadii* is the only known host. Soon after the discovery of ΦCh1 a close relationship to *H. salinarum* virus ΦH was proposed on sequence and protein similarities (KLEIN *et al*., 2002). Protein E of ΦCh1 shares 80 % sequence similarity to the major capsid protein Hp32 of ΦH on amino acid level (KLEIN *et al*., 2000).

ΦCh1 has a typical head-tail morphology with a total length of 200 nm and a contractile tail with a diameter of 20 nm, therefore ΦCh1 belongs to the family of *Myoviridae* (see Figure 4). The particles contain 58,498 bp linear double-stranded DNA as well as RNA (KLEIN *et al.*, 2002), making it the first virus to observe this phenomenon. Until that a fundamental difference between viruses and living organisms was that viruses either contain DNA or RNA but not both (REANNEY & ACKERMANN, 1982). The sequence of ΦCh1 *N. magadii* strain L13, which has been 'cured' of ΦCh1 by multiple passaging, can be reinfected with virus particles leading to turbid plaques. A turbid plaque indicates that ΦCh1 is a temperate virus, meaning it has a lytic and a lysogenic lifecycle. During the lysogenic lifecycle ΦCh1 is integrated in the host genome in contrast to ΦH which remains as a plasmid outside the chromosome (SCHNABEL *et al.*, 1982). The *N. magadii* strain carrying ΦCh1 is named L11. Like its host *N. magadii*, ΦCh1 requires salt concentrations above 2 M NaCl, otherwise the particles lose their morphological stability and infectivity (WITTE *et al.*, 1997).

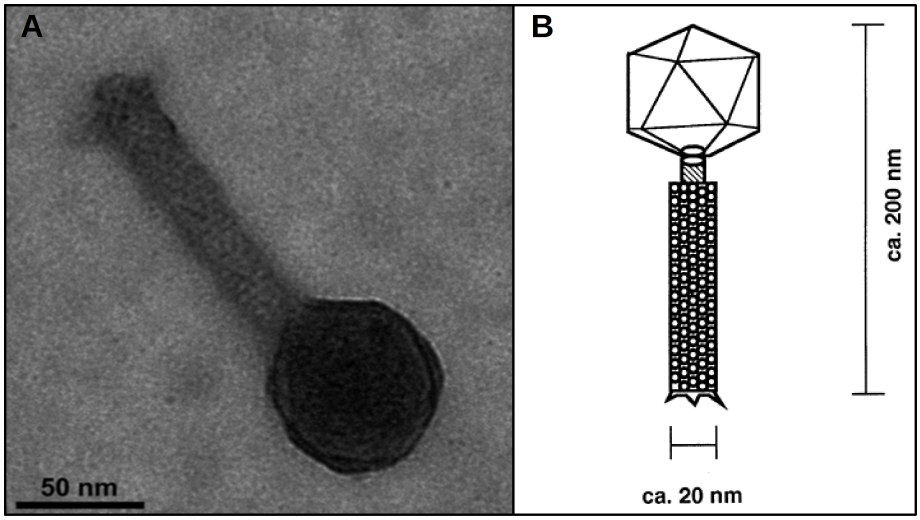

Figure 4: Electron micrograph of ΦCh1 and schematic view. Adapted from Selb et al. 2017 (A) and Witte et al. 1997 (B).

1.2.2.1 Genome organization

The DNA of ΦCh1 is methylated by viral-encoded methyltransferases and has an overall G+C content of 61.9 % (BARANYI *et al*., 2000; KLEIN *et al*., 2002). One of those methyltransferases is ORF94 (Mtase) (HAIDER, 2009). The genome is terminally redundant and circularly permuted, indicating a headful mechanism for packaging DNA into the capsid (KLEIN *et al*., 2002). In 2002 sequencing of ΦCh1 led to the identification of 98 putative open reading frames (ORFs). 48 ORFs match to other ORFs of known function, among them 31 to hypothetical proteins of mostly unknown function that share high sequence similarity to ORFs of ΦH and 17 show similarities to proteins of known function. 50 putative proteins did not match any other proteins (KLEIN *et al*., 2002).

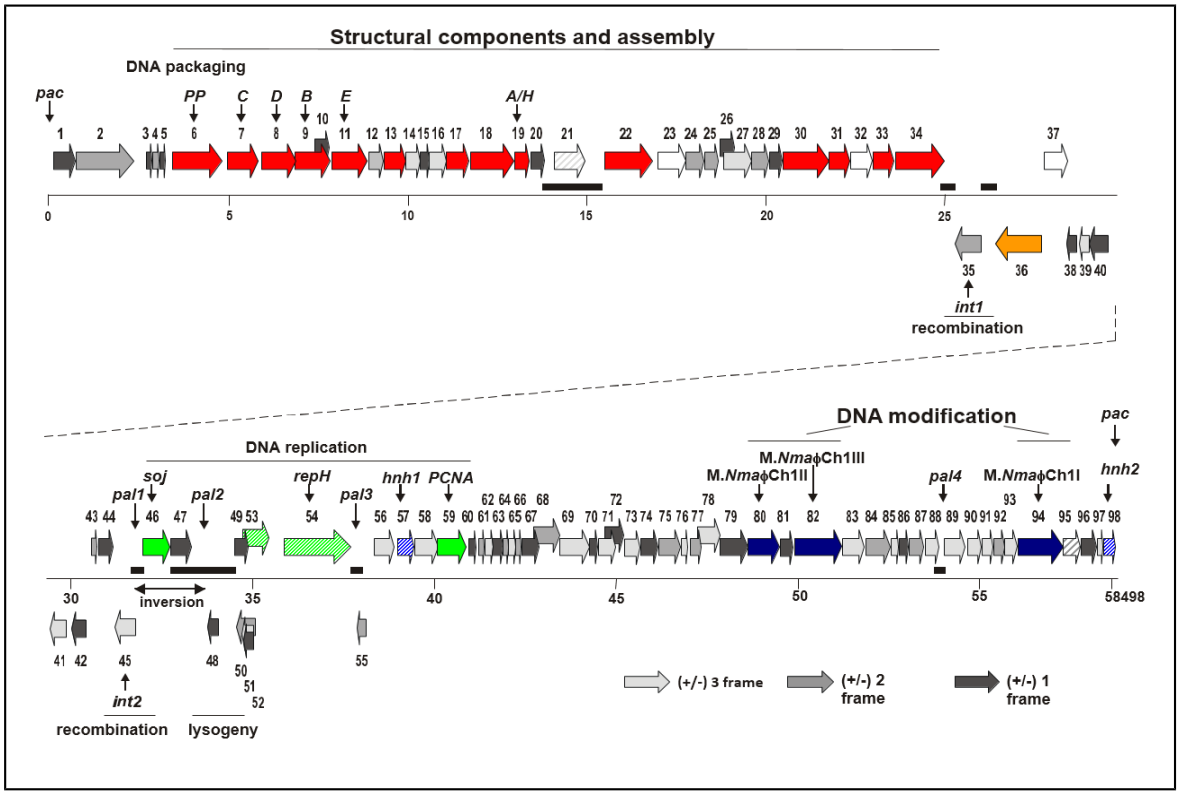

Figure 5: Genome of ΦCh1 with predicted ORFs indicated by arrows. The 5' region is composed exclusively of right-ward transcribed genes responsible for structural components (red arrows) and assembly of virus particles. The middle part consists of left- and right-ward transcribed genes and an invertible region. Identified genes in this module are involved in DNA replication (green arrows). The 3' end again has only right-ward transcribed genes, which encode among others DNA-methyltransferases (dark blue arrows). Adapted from Klein *et al*., 2002.

Bacteriophage genomes are often organized in so called functional modules. Usually genes are not randomly distributed over the genome, instead they are clustered according to their function like DNA packaging, transcriptional regulation or host lysis. The ΦCh1 genome can be divided in three distinct functional modules: structural components and assembly, DNA replication and DNA modification (see Figure 5).

The autonomous replicating plasmid pΦHL, which is a circularized part of ΦH, has a size of about 12 kbp and an overall similarity to the middle part of ΦCh1 (approximately from base 30,000 to 42,000) of at least 50 % up to 97 % (KLEIN *et al*., 2002).

1.2.2.2 Regulation of lytic and lysogenic life cycle

A strict regulation of the lytic and lysogenic life cycle is important for temperate viruses to ensure their survival. Many phages use transcriptional repressors to control life cycle like the bacteriophage λ. Upon sequence comparison ORF48 of ΦCH1 showed similarities to the repressor of ΦH, therefore the gene product of ORF48 (*rep*) was called "Rep" (IRO *et al*., 2007). Rep posseses a winged helix-turn-helix motif which confers the ability to bind to DNA. Together with ORF49 *rep* forms a putative repressor-operator system, thus forming the lysogenic region in ΦCh1 (IRO *et al*., 2007).

1.2.2.3 The operon ORF43/44

ORF43 and ORF44 of ΦCh1 together form a transcriptional unit. They are co-transcribed and co-translated due to the fact that their start and stop codons are overlapping. A typical haloarchaeal promoter sequence is located upstream of ORF43 (SOPPA, 1999). ORF43-44 shows high similarities with two ORFs in ΦH which are co-operative elements of the repressor of ΦH. The repressor *rep* is constitutively expressed throughout the viral life cycle. Therefore there must be another level of regulation to induce the lytic phase of ΦCh1. It was shown that gp43-44 have an enhancing effect on transcription from the ORF49 promoter (IRO *et al*., 2007). This data put the operon ORF43-44 in the spotlight of research. Investigation of gp43 showed no domains of known function, however gp44 has a PIN domain (PilT N terminal domain) according to Pfam analysis (IRO *et al*., 2007). These domains are metal-dependent sequence- or structure-specific endoribonucleases (CRUZ *et al*., 2015; YAMAGUCHI *et al*., 2011), which can be found in all domains of life.

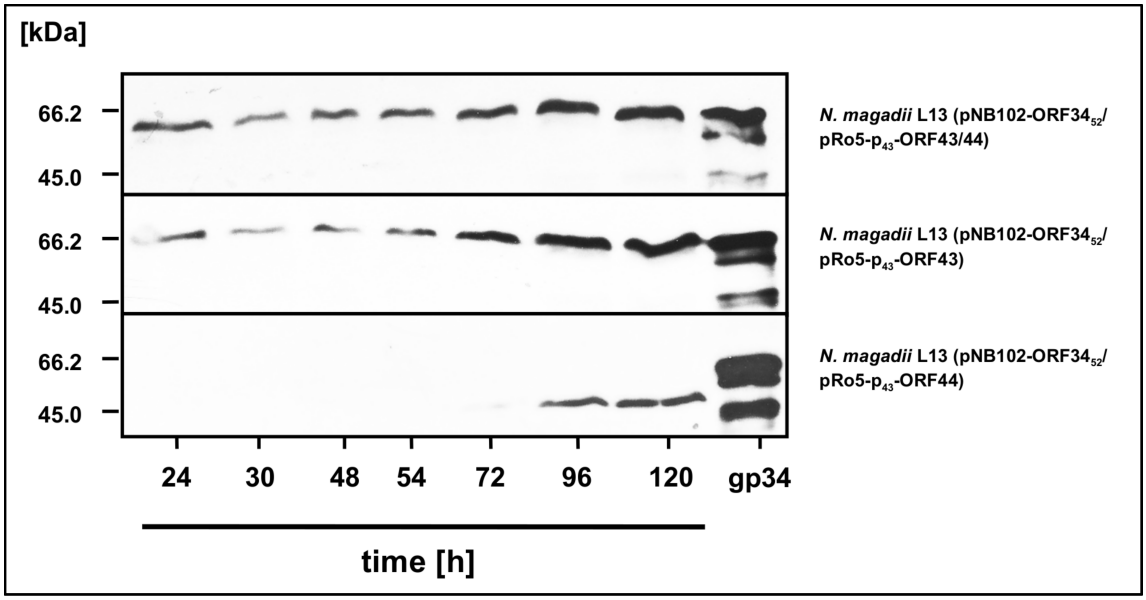

Figure 6: The Western blot shows the expression of ORF3452 in *N. magadii* L13 (pNB102-ORF3452/pRo5-p43-ORF43/44), *N. magadii* L13 (pNB102-ORF3452/pRo5-p43-ORF43) and *N. magadii* L13 (pNB102-ORF3452/pRo5-p43-ORF44). Lane 1-7 represents the different time points where samples were taken. Lane 8: crude protein extract from *E. coli* XL1-Blue (pQE30-ORF3452) as a control. The signal of gp34$_{52}$ with gp43/44 or gp43 does not differ from the control. The expression of gp44 prevents the signal until 48 hours. Cells of *N. magadii* L13 (pNB102-ORF3452/pRo5-p43-ORF44) express ORF34$_{52}$ 96 hours after inoculation of the culture. Here the same intensities were detected as for the other strains. Adapted from Hofbauer, 2015.

The PIN domain consists of about 130 amino acids and can be identified by three strictly conserved acidic residues (ARCUS *et al*., 2011). The amino acids 3 to 126 out of 132 of gp44 show high similarity to the PIN domain consensus sequence (IRO *et al*., 2007).

The regulatory role of gp43 and gp44 was investigated. Therefore experiments in *N. magadii* L13 were performed to characterize gp43 and gp44. *N. magadii* L13 was transformed with two different plasmids. One contained the reporter gene $ORF34_{52}$ and the second one ORF43/44 as an operon, ORF43 or ORF44 alone. As shown in Figure 6, expression of $ORF34_{52}$ did not change in *N. magadii* L13 (pNB102-$ORF34_{52}$/pRo5-p43-ORF43/44) and *N. magadii* L13 (pNB102-$ORF34_{52}$/pRo5-p43-ORF43). However, in the case where only gp44 is present a strong phenotype can be seen. Not only the expression of the reporter gene $ORF34_{52}$ is delayed until 72 hours after inoculation but also a difference in size of about 20 kDa can be seen (HOFBAUER, 2015). This experiment was repeated with Mtase (ORF94) as a reporter gene (see Figure 7). In the upper Western blot (Figure 7A) *N. magadii* L13 (pNB102-ORF94/pRo5-p43-ORF43) an almost constant expression over a time of 8 days was observed. However, *N. magadii* L13 (pNB102-$ORF34_{52}$/pRo5-p43-ORF44) again shows a distinct phenotype (Figure 7B). Expression of the gene is delayed but the gene product is not truncated, instead protein production is extremely reduced (LEBHARD, 2016). This data indicates that the mRNA of $ORF34_{52}$ is cleaved by gp44 within the coding region and the mRNA of Mtase is cleaved

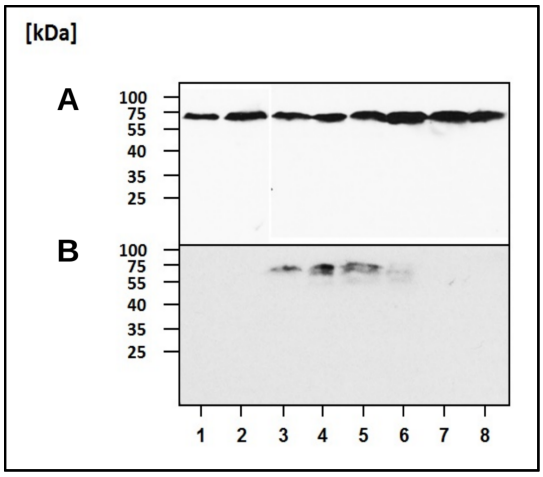

Figure 7: Western blots show the expression of Mtase together with either ORF43 (A) or ORF44 (B). (A) shows a constant expression of Mtase over the whole time span. In (B) a reduced (lane 3-6) or complete inhibition of expression (lane 1, 2, 7 and 8) can be seen. Adapted from Lebhard, 2016 .

within in the 5'-untranslated region (5'-UTR). For this reason, the 5'UTR of Mtase and the coding region of $ORF34_{52}$ were aligned using the "EMBOSS Water Pairwise Sequence Alignment" tool from the EMBL-EBI homepage https://www.ebi.ac.uk/Tools/psa/emboss_water/nucleotide.html (see Figure 8A). The result confirms the presumption that those two genes may have a common restriction site for gp44. However, due to the lack of experimental data it is still unknown whether gp44 is a RNase or if it cleaves RNA sequence- or structure specifically. Therefore the putative recognition sequence (underlined in Figure 8) is an assumption and may not be the exact cleavage site. A seven basepair cleavage site is also found in the halophilic archaeon *Haloquadratum walsbyi* (YAMAGUCHI *et al*., 2012). Nevertheless, the 5'-UTR of Mtase was compared to other ORFs of ΦCh1. Among others two promising matches show the same sequence: first ORF22, the minor capsid protein (Figure 8B), second ORF11 the major capsid protein of ΦCh1 (Figure 8C). While in ORF11 the same putative sequence like in $ORF34_{52}$ can be found, ORF22 has exactly the same sequence CGGTTAC. Therefore both of them can be used to identify more putative targets of gp44.

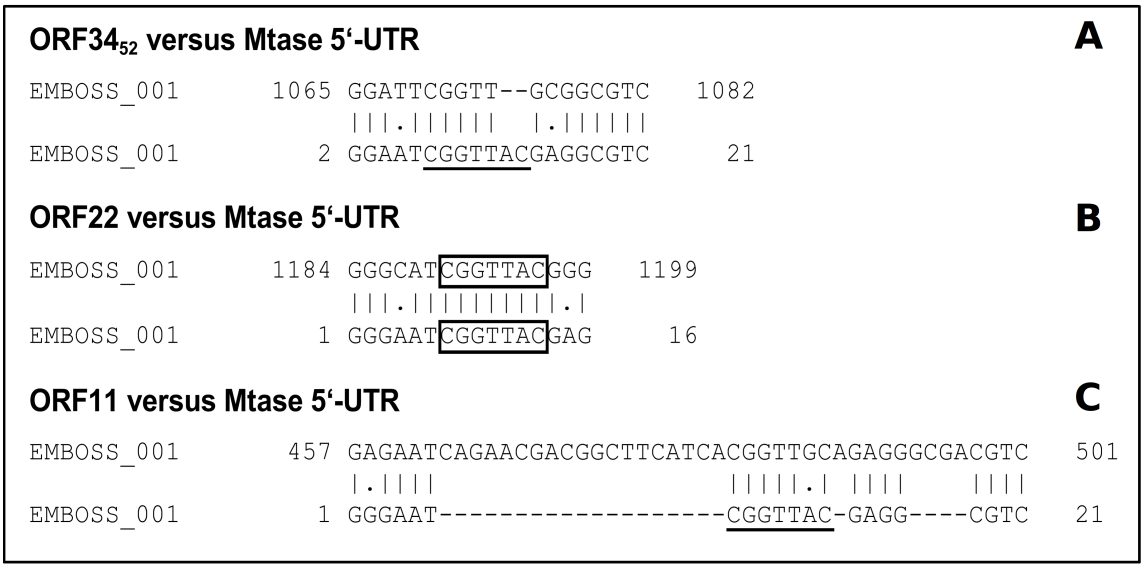

Figure 8: Sequence comparison of Mtase 5'-UTR with ORF3452 (A), ORF22 (B) and ORF11 (C).

1.3 Toxin-Antitoxin systems

Toxin-Antitoxin systems (TA-systems) are small genetic modules that can be found in all domains of life. They consist of a stable toxin and an unstable antitoxin which can regulate the toxin. In many cases overproduced or unregulated toxins lead to cell death. Therefore homeostasis of toxin and antitoxin by constitutive replenishment of antitoxin is essential for the survival of the cell. The first TA-system was described as a plasmid maintenance system (GERDES *et al.*, 1990). This system prevents the formation of plasmid free cells. After segregation the labile antitoxin is degraded and cannot be produced again therefore the stable toxin will kill the cell. This mechanism is called post-segregational killing (PSK). Until now two additional biological functions have been shown for TA-toxins. One is bacterial abortive infection (DY *et al.*, 2014), the other one is formation of persister cells (HARMS *et al.*, 2016). If a bacterial cell gets infected by a bacteriophage, abortive infection systems lead to an altruistic cell death to prevent spread of new phages. Persister cells are a subpopulation of cells in a bacterial population. These cells exhibit tolerance to environmental stress conditions like antibiotics or starvation. This dormant state is caused by self-poisoning with a toxin which inhibits vital cellular process. Figure 9 shows the different molecular targets of vital processes, like translation, which can be inhibited by TA-encoded toxins. Until now 6 types of TA-systems have been

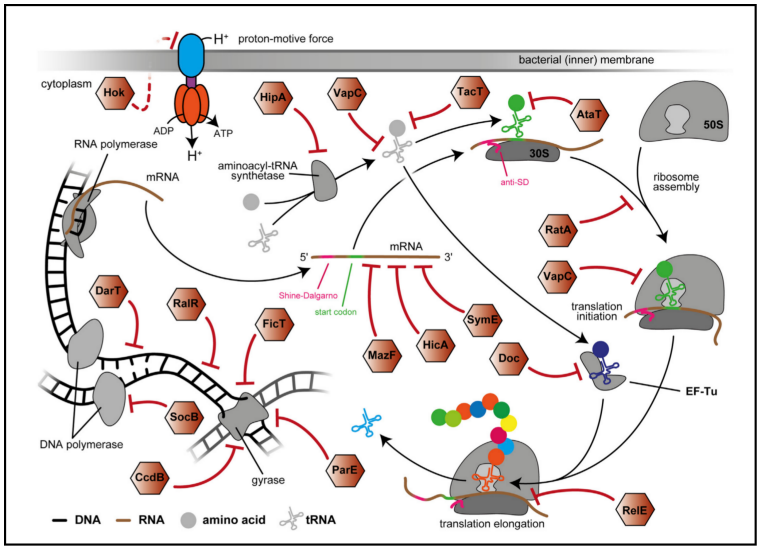

Figure 9: Molecular interference in vital processes of selected TA-encoded toxins. Adapted from Harms *et al.*, 2018.

characterized (HARMS *et al*., 2018). These types differ in the way toxin neutralization. PIN-domains, like in gp44, are found in the VapBC (virulance associated proteins) family of type II TA-systems (ARCUS *et al*., 2011).

1.3.1 The type II TA-system and the VapBC family

The type II TA-systems are the most extensively studied among them. The best studied families of these toxins are MazEF (AIZENMAN *et al*., 1996), RelBE (PEDERSEN *et al*., 2003), YefM/YoeB (KAMADA & HANAOKA, 2005; ZHANG & INOUYE, 2009), MqsAR (KASARI *et al*., 2010; YAMAGUCHI *et al*., 2009), HicAB (MAKAROVA *et al*., 2006) and, the most abundant one, VapBC (ROBSON *et al*., 2009). The antitoxin interacts directly as a protein with its cognate toxin and blocks the toxic activity of the toxin. The genes are usually arranged in an operon and have either overlapping start and stop codons or are in close proximity of each other, where in vast majority of cases the antitoxin is located upstream of the toxin. The main characteristic feature of the VapC toxin is the presence of the PIN-domain and the majority of these domains in prokaryotes are part of a TA-system. PIN-domains are Mg^{2+}- or Mn^{2+}-dependent ribonucleases and can cleave either in a sequence- or structure-specific manner. However, the exact mechanism and the specific targets remain unknown. PIN-domains are identified by the presence of three strictly conserved acidic amino acid residues, but the rest of the around 130 amino acids show only poor similarities (ARCUS *et al*., 2011). Nevertheless, the structural fold, which locates the conserved amino acids in the active center together with a serine or threonine as the coordinator for Mg^{2+} or Mn^{2+}, is conserved (ARCUS *et al*., 2011; LEVIN *et al*., 2004).

1.3.2 Regulation of type II TA-systems

There are two steps at which TA-systems can be regulated: transcription and translation. Transcriptional regulation can be achieved by integration of TA-modules into cellular signaling pathways, like the SOS-response (DÖRR *et al.*, 2010). Type II TA-systems are usually controlled via transcriptional autoregulation. In most cases they are expressed from one single promoter upstream of the locus, that is repressed by binding of either the antitoxin alone or the TA complex (BROWN *et al.*, 2013; GOTFREDSEN & GERDES, 1998). Other TA-systems rely on a similar mode of action that is called "conditional cooperativity". The regulation of these systems is based on the stoichiometry of toxin and antitoxin. The mechanism for this can be seen in Figure 10 (CHAN *et al.*, 2016). Different ratios of toxin (Kid) to antitoxin (Kis) lead to different formation of complexes of toxin

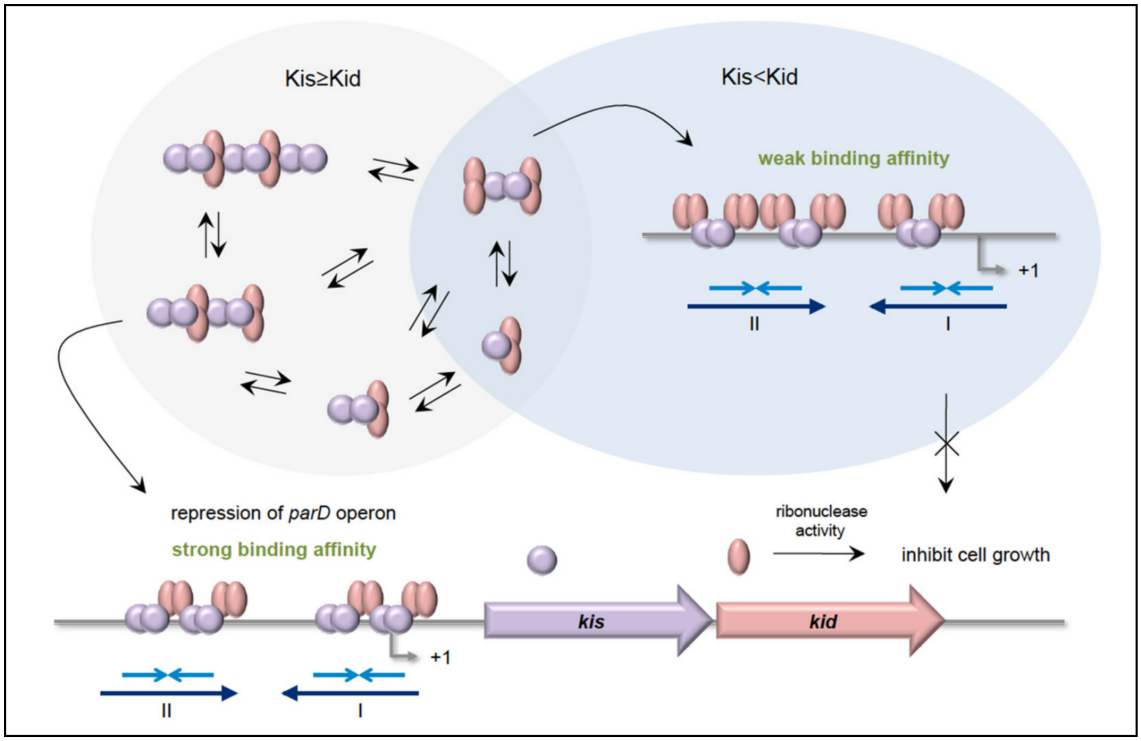

Figure 10: Stoichiometries of Kis-Kid complexes and their binding affinities to parD DNA. When the Kis antitoxin is in excess, or in equal amounts as Kid toxin, various Kis-Kid complexes are formed (e.g., [Kid 2-Kis 2]$_n$ or [Kid 2-Kis 2-Kid 2-Kis 2]$_n$ etc.). The most abundant one, the Kid 2-Kis 2-Kid 2-Kis 2 octamer complex, binds strongly to the two half-sites of the parD DNA regions I and II with two Kis dimers, and thus strongly represses the transcription of parD operon. When the Kid toxin exceeds Kis antitoxin, the Kid 2-Kis 2-Kid 2 hexamer is the most abundant. The Kid 2-Kis 2-Kid 2 hexamer has weak affinity toward parD DNA as it can only bind to the two half-sites of regions I and II using one dimer. Adapted from Chan *et al.*, 2016.

and antitoxin. Excess of Kid leads to formation of the hexameric Kid 2-Kis 2-Kid 2, which has a weak binding affinity for the promoter region of the parD operon. However, if more antitoxin is present, the octamer Kis 2-Kid 2-Kis 2-Kid 2 is most abundant. This complex has a strong affinity and can repress the operon (DIAGO-NAVARRO *et al*., 2010; M. KAMPHUIS *et al*., 2007; M. B. KAMPHUIS *et al*., 2007; MONTI *et al*., 2007). This system also ensures that persister cells can go back to a normal state by changing the ratio of toxin to antitoxin.

In many cases the instability of the antitoxin can be explained by the "disorder-order" binding model. In this model an unstructured antitoxin, which is a preferential target of cellular proteases, will fold in a well organized structure upon binding to its cognate toxin and getting more stable. Examples are the CcdAB and YefM/YoeB loci from *E. coli* (CHERNY & GAZIT, 2004; DE JONGE *et al*., 2009, 2010; KAMADA & HANAOKA, 2005). However, there are also antitoxin with a distinct secondary or tertiary structure without being bound to the toxin: MqsAR from *E. coli* (BROWN *et al*., 2009) and YefM/YoeB from *Mycobacterium tuberculosis* (KUMAR *et al*., 2008). With constant expression of antitoxin the level of possible active toxin is kept at a minimum. The toxin gets activated upon proteolytic degradation of the antitoxin, if the cell encounters environmental stress.

It was reported that TA-systems can regulate other TA-systems (WANG *et al*., 2012). The MqsR endoribonuclease toxin cleaves the antitoxin part of the ghoS-ghoT mRNA. Therefore, activation of MqsR leads to activation of GhoT by repressing the expression of GhoS. Trans-activation of TA-systems by overexpression of other TA-systems was reported (GARCIA-PINO *et al*., 2008; WINTHER & GERDES, 2009), however the general mechanism underlying trans-activation is still unknown. It is possible that trans-activation

is just a secondary effect of translation inhibition by TA-systems, rapid degradation of the antitoxin.

1.4 Aim of this thesis

The aim of this thesis was to further investigate the putative TA-system ORF43/44 of ΦCh1. In 2007 IRO *et al*. hypothesized that the operon ORF43/44 is a TA-system, because it showed significant similarities to the VapBC family of type II TA-systems. HOFBAUER and LEBHARD showed that gp44 has an effect on $gp34_{52}$ and Mtase respectively, however it is unknown if this is due to cleavage of mRNA or proteolytic cleavage or degradation of the reporter gene (HOFBAUER, 2015).

Since ORF43/44 may be involved in regulation of the lysogenic life cycle, in 2017 GILLEN constructed an ORF44 deletion mutant in order to characterize ORF44 in its native host *N. magadii* alongside with the viral background. He observed a 24 hours earlier onset of lysis, however the lysis kinetics showed no significant difference to *N. magadii* L11. As he carried out outgrowth experiments with subsequent Western blot analysis of protein kinetics, he observed that expression of the reporter genes was delayed at least 48 hours compared to *N. magadii* L11. The reporter genes used were ORF11, which encodes for the major capsid protein, $ORF34_{52}$ and Mtase. GILLEN also observed that the deletion mutant returned after four to five passages to the cured strain *N. magadii* L13, indicating that the provirus is not stable (GILLEN, 2017).

EDWARDS did further investigation of the ORF44 deletion mutant regarding stability of the provirus. She analyzed in total 8 passages and observed the same phenomenon. After the 5^{th} passage the growth behavior was comparable to that of the cured strain *N. magadii* L13. One possibility is that due to the lack of the toxin gp44 the putative addiction module got

lost, therefore with continuous passaging mutations can accumulate and the virus becomes unstable. Reinfection of cells of the 8th passage was observed, indicating the "cured state" of the cells (EDWARDS, 2018).

The aim of this thesis was to elucidate the regulation of the putative TA-system ORF43/44. Therefore the putative autoregulatory function of gp43 was investigated. Additionally, based on the sequence alignments identification of other putative targets of gp44, like ORF11 and ORF22, was the major goal. Within this experiment the role of ORF22 was examined. Furthermore, as it is known that gp44 has an impact on ORF34$_{52}$, the putative recognition site was intended to be mutated. If the full-length protein is still detectable in Western blot analysis, the information supports the hypothesis, that gp44 is a sequence-specific endoribonuclease. Detailed experimental setup is described in part 3 "Results and discussion".

2 Material and Methods

2.1 Material

2.1.1 Bacterial and archaeal strains

Escherichia coli

Strain	Modifications	Source
XL-1 Blue	*recA1*, *endA1*, *gyrA96*, *thi-1*, *hsdR17*, *supE44*, *relA1*, *lac* [*F' proAB lacI^q ZΔ M15* Tn10 (Tet^R)]	Stratagene
Tuner	*dcm, ompT, hsdS*($r_B^-m_B^-$) *gal*, *lacY1*, λ(DE3)	Novagen
Rosetta(DE3)pLysS	*Dcm*, *ompT*, *hsdS*($r_B^-m_B^-$), *gal*, λ(DE3) pLysSRARE(Cam^R)	Novagen
BL21(DE3)pLysS	*dcm*, *ompT*, *hsdS*($r_B^-m_B^-$), *gal,* λ(DE3), pLysS(Cam^R)	Novagen

Natrialba magadii

Strain	Modifications	Source
L13	Cured strain; does not contain ΦCh1 anymore	WITTE *et al*., 1997
L11	Carries the virus ΦCh1 in the genome as a provirus	WITTE *et al*., 1997

2.1.2 Growth media

2.1.2.1 Lysogeny broth medium (LB-medium)

NaCl.....5 g
Yeast extract.....5 g
Peptone.....10 g

pH 7, ddH_2O ad 1 l, for plates: 15g/l agar; autoclave

2.1.2.2 Rich medium for haloalkalophilic *Archaea* (NVM$^+$)

NaCl.....235 g
KCl.....2.35 g
Yeast extract.....11.7 g
Casamino acids .....8.8 g
Sodium citrate tribasic dihydrate.....0.8 g

pH 9-9.5, ddH_2O ad 935 ml, for plates: 10 g/l agar for plates; autoclave

After autoclaving complement with:

0.57 M Na_2CO_3 (dissolved in sterile ddH_2O).....63 ml
1 M $MgSO_4$ (autoclaved) ….....1 ml
20 mM $FeSO_4$ (dissolved in sterile ddH_2O).....1 ml

2.1.2.3 Natrialba mineral medium b (NMMb$^+$)

NaCl.....205 g
KCl.....2 g
Na_2HPO_4.....0.28 g
NaH_2PO_4.....0.28 g
Alanin.....2.23 g
Leucin.....0.66 g
Arginin.....0.81 g
Histidin.....0.778 g
Lysin.....0.731 g
Sodium citrate tribasic dihydrate.....0.8 g
Sodium acetate.....1.66 g
Sodium pyruvate.....1.1 g

pH 9-9.5, ddH_2O ad 900 ml, for plates: 8 g/l agar for plates; autoclave

After autoclaving complement with:

1.75 M Na_2CO_3 (dissolved in sterile ddH_2O).....100 ml
1 M $MgSO_4$ (autoclaved) .....1 ml
20 mM $FeSO_4$ (dissolved in sterile ddH_2O).....250 µl
1,000x trace elements.....1 ml

2.1.2.3.1 1000x trace elements

$MnCl_3$ .....93 mg
$CaCl_2$.....44 mg
$CuSO_4$.....64 mg
$ZnSO_4$.....64 mg

ddH_2O ad 100ml, autoclave

2.1.3 Additives

Compound	Stock concentration	Final concentration	Preparation
IPTG	1 M	1 mM	Dissolved in ddH_2O, sterile filtered, stored at -20°C
Ampicillin	20 mg/ml	100 µg/ml	Dissolved in ddH_2O, sterile filtered, stored at 4°C
Tetracyclin	10 mg/ml	10 µg/ml	Dissolved in half the volume ddH_2O, followed by half the volume of 96 % ethanol, stored at -20°C, light protected
Chloramphenicol	40 mg/ml	20 mg/ml	Dissolved in 96 % ethanol, stored at -20°C
Mevinolin*)	10 mg/ml	7.5 µg/ml	Isolated from pulverized tablets, dissolved in 96 % ethanol, stored at -20°C
Novobiocin	3 mg/ml	3 µg/ml	Dissolved in ddH_2O, sterile filtered, stored at -20°C, light protected
Bacitracin	7 mg/ml	70 µg/ml	Dissolved in ddH_2O, sterile filtered, stored at 4°C, light protected
Tryptophan	0,6 M	2 mM	Dissolved in 1 M NaOH, stored at -20°C, light protected

*) Mevinolin was isolated from tablets containing 20 mg mevinolin each. The tablets were pulverized and subsequently dissolved in 96 % ethanol. The solution was stirred gently for 20 minutes. Afterwards the solution was centrifuged for 20 minutes with 12.000 rpm at 4°C. The supernatant was collected.

2.1.4 Plasmids

Construct	Features	Source
pBlueScriptII KS (+)	*bla*, ColE1 ori, *mcs*, *lacZα*	Stratagene
pQe16	*bla*, ColE1 ori, C-terminal 6x His-tag	Qiagen
pQE30	*bla*, ColE1 ori, N-terminal 6x His-tag	Qiagen
pRSET-A	*bla*, pUC ori, T7 promoter, N-terminal 6x His-tag	Invitrogen
pRo5	*bla*, ColE1 ori, *gyrB* (Nov^R), ΦCh1 derived ori	MAYRHOFER-IRO *et al*., 2013
pNB102	*bla*, ColE1 ori, *hmg* (Mev^R), pNB101 ori	ZHOU *et al*., 2004
pKS-p43	pKS with promoter of ΦCh1 ORF43/44 operon	SCHMAL, 2016
pKS-p34	pKS with promoter of ΦCh1 ORF34	Laboratory stock
pRV1-pTna	*bla*, pMB1, pHK2, *gyrB*, ptna (Hfx. Volcanii), *bgaH*	LARGE *et al.*, 2007
pKS-p43-bgaH	pKS with bgaH under promoter of ΦCh1 ORF43/44 operon	This thesis
pNB102-p43-bgaH	pNB102 with bgaH under promoter of ΦCh1 ORF43/44 operon	This thesis
pRo5-p43-ORF43	pRo5 with ORF43 under its native promoter	MEISSNER, 2008
pNB102-p34-ORF22	pNB102 with ORF22 under promoter of ORF34	MAIR, 2017
pRo5-p43-ORF44	pRo5 with ORF44 under its own promoter	MEISSNER, 2008
pRo5-pTna-ORF44	pRo5 with ORF44 under	TSCHURTSCHENTHALER, 2015

Construct	Features	Source
	the inducible tryptophanase promoter	
pNB102-p34-ORF11	pNB102 with ORF11 under promoter of ORF34	This thesis
pNB102-M-Eco-12	pNB102 with substitution mutant of $ORF34_{52}$	This thesis
pRSET-A-ORF22	pRSET-A with ORF22	This thesis
pQE30-ORF19	pQE30 with ORF19	Laboratory stock
pQE16-ORF22	pQE16 with ORF22	This thesis
pQE30-ORF22	pQE30 with ORF22	This thesis
pRSET-A-ORF22-N	pRSET-A with N-terminus of ORF22	This thesis
pQE30-ORF22-N	pQE30 with N-terminus of ORF22	This thesis

2.1.5 Kits

Name	Manufacturer	Product number
Wizard® Plus SV Minipreps DNA Purification System	Promega	A1460
Wizard® SV Gel and PCR Clean-Up System	Promega	A9282
SuperSignal® West Pico Chemiluminescent Substrate	Thermo Scientific	34080
QIAquick® Gel Extraction Kit	Qiagen	28706
Monarch™ PCR & DNA Cleanup Kit (5µg)	New England BioLabs	T1030G
Gibson Assembly® HiFi 1-Step Kit	Synthetic Genomics	GA1100-02

2.1.6 Primer

Name	Sequence	Restriction site
pKS-p43-BgaH_F	CGGCCGGTTTAAAGCTTCTTGGCCGCTCTAGAACTAGTGG	/
pKS-p43-BgaH_R	ACTCTTCACACGCGGTACCTTCGAGGTCGACGGTATCGAT	/
BgaH-3i	GAGTGAAAAACCACCCATG	/
43-5up-H	GATTAAGCTTGTTGTGCCAGCCGTCGA	*Hind*III
E-Kpn-2	GTTAGGTACCTTACGAGGTCTCCTCTTCGAGG	*Kpn*I
E-BgI-2	GACCAGATCTATGGCATCCCGAACCAT	*Bgl*II
36-3X	GCAGTCTAGACCATCGGTTATTCGAGTTTC	*Xba*I
M-Eco-34-1	GTGGATTCGAATTCGGCGTCCATCATCGC	*Eco*RI
34-Kpn	CAGCAGGGTACCCGGCGTTCGAGGTCA	*Kpn*I
M-Eco-34-2	GTATGAATTCGAATCCATCGCCGTCTG	*Eco*RI
22-Bam	CAGACGGATCCATGATTCCAGGAGGAG	*Bam*HI
22-N-Hind	GAACAAGCTTTCACACTGTCTCGTTCCACTC	*Hind*III
22-N-Bgl	GAACAGATCTCACTGTCTCGTTCCACTC	*Bgl*II
22-Bgl	CAGCAGAGATCTGCGCAGCAGTCGCC	*Bgl*II

2.1.7 Enzymes

PCR

Name	Manufacturer	Product number	Details
Pfu DNA Polymerase	Promega	M7741	Used for cloning
GoTaq DNA polymerase/*GoTaq* Green Mastermix	Promega	M3001/M7123	Used for analytical amplifications
Phusion DNA polymerase/High-Fidelity PCR Master Mix with HF Buffer	Thermo Scientific	F531	Used for cloning

All polymerases were used with the provided kit-specific reaction buffers.

Restriction digest

Restriction enzymes for conventional restriction digest were provided by Thermo Scientific. Buffers were selected according to manufacturer's recommendation. For double digestions buffers were used according to Thermo Scientific DoubleDigest Calculator.

Other enzymes

Name	Manufacturer	Product number	Details
T4 DNA ligase	Promega	M1808	Used for cloning
Proteinase K	Qiagen	19133	Used for *N. magadii* competent cells

2.1.8 Size Markers

DNA marker

Marker	Manufacturer	Product number	Fragments(bp)
λ-*Bst*EII	Thermo Scientific (λ-DNA and *Bst*EII)	SD0011 (λ DNA) ER0391 (*Bst*EII)	8454, 7242, 6369, 5686, 4822, 4324, 3675, 2323, 1929, 1371, 1264, 702

Protein Marker

Marker	Manufacturer	Product number	Fragments(kDa)
PageRuler™ Prestained Protein Ladder	Thermo Scientific	26616	180, 130, 95, 72, 55, 43, 34, 26, 17, 10

2.1.9 Antibodies

Primary antibodies

Antibody	Target	Application	Source
α-ΦCh1 (rabbit)	Whole capsid of ΦCh1	Diluted 1:1500 in 1x TBS, 0.3 % BSA, 0.02 % NaN_3	Laboratory stock
α-E (rabbit)	Protein E of ΦCh1	Diluted 1:2500 in 1x TBS, 0.3 % BSA, 0.02 % NaN_3	Laboratory stock
α-His (6-His: His-Tag unconj., mouse)	His-Tag	Diluted 1:5000 in 1x TBS, 0.3 % BSA, 0.02 % NaN_3	Dianova
α-22-N (rabbit)	N-terminal part of gp22 of ΦCh1	Diluted 1:2000 in 1x TBS, 0.3 % BSA, 0.02 % NaN_3	This thesis Immunization: Moravian-Biotechnology Ltd

Sedondary antibodies

Antibody	Target	Application	Source
α-mouse IgG, horseradish peroxidase linked (sheep)	Mouse IgG	Diluted 1:5,000 in 1x TBS	GE Healthcare
α-rabbit IgG, horseradish peroxidase linked (donkey)	Rabbit IgG	Diluted 1:5,000 in 1x TBS	GE Healthcare

2.1.10 General buffers and solutions

2.1.10.1 Buffers for DNA methods

50x TAE

Tris-HCl pH 8.2.....2 M
Acetic acid.....1 M
EDTA.....0.1 M

6x DNA loading dye

Orange G.....0.144 % m/v
Xylene Cyanol.....0.036 % m/v
Tris-HCl pH 8.0.....0.25 M
Glycerol.....60 %

Ethidium bromide bath

Ethidium bromide.....10 µg/ml

Agarose for gels was melted in 1x TAE.

2.1.10.2 Buffers for protein methods

10x SDS-running buffer

Tris.....0.25 M
Glycine.....1.92 M
SDS.....1 %

4x Stacking gel buffer

Tris-HCl pH 6.8.....0.5 M
SDS.....0.4 %
autoclaved

4x Separating gel buffer

Tris-HCl pH 8.8.....1.5 M
SDS.....0.4 %
autoclaved

30 % acrylamide

Acrylamide .....29 %
N,N'-methylenbisacrylamide.....1 %

2x Laemmli sample buffer

Tris-HCl pH 6.8.....0.12 mM
SDS.....2 %
Glycerol.....17.4 %
β-mercaptoethanol.....2 %
Bromphenolblue.....0.02 %

100 ml 1 M phosphate buffer pH 6.8

1 M Na_2HPO_4.....46.3 ml
1 M NaH_2PO_4.....53.7 ml

Coomassie staining solution

Methanol.....25 %
Acetic acid.....10 %
Coomassie Brilliant Blue R-250.....0,15 %

Destaining solution

Acetic acid .....10 %

Blocking solution

5 % milk powder in 1x TBS

10x PBS

NaCl.....1.37 M
KCl.....27 mM
NaH_2PO_4.....14.7 mM
Na_2HPO_4.....81 mM
pH 7.4

10x TBS

Tris-HCl pH 8.0.....0.25M
NaCl.....1.37M
KCl.....27mM

Transblot buffer

Tris.....48mM
Glycine.....39mM
SDS.....0.034 %
Methanol.....20 %

Buffer B

Na_2HPO_4.....100 mM
Tris.....10 mM
Urea.....8 M
pH adjusted to 8.0 prior to use

Buffer C

Na_2HPO_4.....100 mM
Tris.....10 mM
Urea.....8 M
pH adjusted to 6.3 prior to use

Buffer D

Na_2HPO_4.....100 mM
Tris.....10 mM
Urea.....8 M
pH adjusted to 5.9 prior to use

Buffer E

Na_2HPO_4.....100 mM
Tris.....10 mM
Urea.....8 M
pH adjusted to 4.5 prior to use

2.1.10.3 Buffers for *E. coli* methods

MOPS I

Mops.....100 mM
$CaCl_2$.....10 mM
RbCl.....10 mM

pH adjusted to 7.0 with KOH

MOPS II

Mops.....100 mM
$CaCl_2$.....70 mM
RbCl.....10 mM

pH adjusted to 6.5 with KOH

MOPS IIa

Mops.....100 mM
$CaCl_2$.....70 mM
RbCl.....10 mM
Glycerol.....15 %

pH adjusted to 6.5 with KOH

2.1.10.4 Buffers for *N. magadii* methods

Buffered high salt spheroplast solution + glycerol

Tris-HCl pH 9.5.....50 mM
NaCl.....2 M
KCl.....27 mM
Glycerol.....15 %

After autoclaving, sterile filtered sucrose was added to final concentration of 15 %

Buffered high salt spheroplast solution

Tris-HCl pH 9.5.....50 mM
NaCl.....2 M
KCl.....27 mM

After autoclaving, sterile filtered sucrose was added to final concentration of 15 %

Unbuffered high salt spheroplast solution

NaCl.....2 M
KCl.....27 mM

After autoclaving, sterile filtered sucrose was added to final concentration of 15 %

bgaH buffer

NaCl.....2.5 M
Tris pH 7.2.....50 mM
$MnCl_2$.....10 µM
β-mercaptoethanol*).....0.1 %

*) added freshly before use

2.2 Methods

2.2.1 DNA methods

2.2.1.1 Agarose gel electrophoresis

DNA fragments larger than 400 bp were separated via a 0.8 % agarose gel.

2.2.1.2 Staining and visualization of DNA

Visualization of DNA was done with ethidium bromide (10 µg/ml in ddH_2O).

2.2.1.3 Preparative PCR

2.2.1.3.1 *Pfu* polymerase

Pfu polymerase was used for preparative PCR due to proofreading activity.

10x *Pfu* buffer	10 µl
Pfu polymerase (2-3 U/µl)	2 µl
Primer 1 (0.05 µg/µl)	5 µl
Primer 2 (0.05 µg/µl)	5 µl
2 mM dNTP mix (0.2 mM)	10 µl
ddH_2O	67 µl
DNA template	1 µl
	= 100 µl

Program

Step	Temperature [°C]	Time [min]	Number of cycles
Initial denaturation	95	5	1
Denaturation	95	1	35
Annealing	T_A	1	
Elongation	72	t	
Final elongation	72	2 x t	1

T_A … melting temperature decreased by 4°C; t … length of fragment divided by 500

2.2.1.3.2 *Phusion* polymerase

Phusion polymerase was used for the amplification of large fragments (above 3 kb).

Phusion Master Mix High Fidelity	25 µl
ddH_2O	17.5 µl
Primer 1 (0.05 µg/µl)	2.5 µl
Primer 2 (0.05 µg/µl)	2.5 µl
DMSO	1.5 µl
DNA template	1 µl
	= 50 µl

Program

Step	Temperature [°C]	Time [sec]	Number of cycles
Initial denaturation	98	30	1
Denaturation	95	10	35
Annealing	T_A	30	
Elongation	72	t	
Final elongation	72	2 x t	1

T_A … melting temperature decreased by 4°C; t … length of fragment divided by 17.

5 µl of PCR product were mixed with 5 µl DNA loading dye and loaded to a 0.8 % agarose gel in order to control the quality.

2.2.1.4 Analytical PCR

Analytical PCR was used to confirm the correct construction of plasmids and the success of transformations.

2x GoTaq® Green Master Mix	12.5 µl
Primer 1 (0.1 µg/µl)	1.5 µl
Primer 2 (0.1 µg/µl)	1.5 µl
DNA template	1 µl
ddH_2O	8.5 µl
	= 25 µl

Program

Step	Temperature [°C]	Time [sec]	Number of cycles
Initial denaturation	95	180	1
Denaturation	95	30	25
Annealing	T_A	30	
Elongation	72	t	
Final elongation	72	2 x t	1

T_A … melting temperature decreased by 4°C; t … length of fragment divided by 17

2.2.1.5 PCR templates

As a DNA template either purified DNA in form of plasmids or crude extracts from cells were used.

2.2.1.5.1 Template from *E. coli*

For analytical PCR 1 µl of culture was used directly.

2.2.1.5.2 Template from *N. magadii*

100 µl culture were centrifuged for 5 minutes at 20,000 g using a tabletop centrifuge. The supernatant was removed, the pellet was resuspendend in 100 µl autoclaved ddH_2O and subsequently denatured at 95°C for 10 minutes.

2.2.1.6 DNA gel elution

In cases where many unspecific products were amplified during the PCR, the fragment was eluted from a 0.8 % agarose gel. After separation the QIAquick® Gel Extraction Kit was used to elute the DNA from the gel.

2.2.1.7 DNA restriction

All restrictions were performed at 37°C for three hours. For vector restrictions DNA concentration was estimated on an agarose gel or by measuring DNA concentration using a spectrophotometer and diluted if necessary. Restriction was controlled on an agarose gel with unrestricted plasmid as negative control.

2.2.1.8 DNA ligation

All ligations were performed at 4°C overnight.

2.2.1.9 Gibson Assembly®

The Gibson Assembly® was performed following the manufacturer's recommendations.

2.2.1.10 DNA purification

2.2.1.10.1 Purification of PCR fragments

After analyzing the PCR on a 0.8 % agarose gel, the DNA fragments were purified to remove all remaining PCR reagents. For that the Wizard® SV Gel and PCR Clean-Up System was used according to the manufacturer's recommendations. DNA was eluted in ddH_2O.

2.2.1.10.2 Purification of plasmid DNA

For plasmid isolation the Wizard® Plus SV Minipreps DNA Purification System was used. Usually 3 ml of fresh overnight culture were used to isolate the plasmid from the cells. After isolation the concentration was measured using a spectrophotometer. DNA was eluted in ddH_2O.

2.2.2 Protein methods

2.2.2.1 Purification of His-tagged protein from *E. coli*

An *E. coli* expression strain was inoculated from an overnight culture to an OD_{600} of 0.1 and incubated on 37°C. As soon as the culture reached the exponential growth phase around an OD_{600} of 0.3 the protein production was induced by adding IPTG. After three hours the culture was centrifuged for 15 minutes with 6,000 g at 4°C and the pellet was frozen overnight at -20°C. Subsequently the cells were thawed on ice for 15 minutes and the pellet resuspended in Buffer B in order to lyse the cells. To complete lysis, the cells were stirred overnight gently to avoid foaming. The next day, the cells were analyzed by light-microscopy whether all of them were lysed. If not, the cells were sonicated until over 95 % of the cells were lysed. The lysate was centrifuged for 20 minutes with 10,000 g at room temperature. The supernatant was mixed with Ni-NTA in order to purify the protein using affinity chromatography. The mixture was stirred overnight gently. Afterwards the Ni-NTA-solution was loaded onto 20 ml column and the flowthrough was collected. The column was washed with Buffer C two times. Proteins were eluted by adding 0.5 ml Buffer D four times and 0.5 ml Buffer E four times. All fractions were analyzed with an SDS-PAGE and finally with a Western Blot. Positive fractions were pooled and dialyzed against 1x PBS for one hour and after changing the buffer overnight. Purified proteins were stored at -20°C.

2.2.2.2 Crude extract protein samples for SDS-PAGE

2.2.2.2.1 *E. coli*

1.5 ml of culture were centrifuged for 5 minutes with 20,000 g at room temperature. The supernatant was discarded and the pellet resuspended in (75*OD_{600}) µl of 5 mM sodium-phosphate buffer and 2x Laemmli buffer. The sample was stored at -20°C.

2.2.2.2.2 *N. magadii*

1.5 ml of culture were centrifuged for 5 minutes with 20,000 g at room temperature. The supernatant was discarded and (75*OD_{600}) µl of 5 mM sodium-phosphate buffer and 2x Laemmli buffer were added without resuspending the pellet. The samples were incubated at 37°C overnight and inverted from time to time. Due to the high copy number of chromosomes the sample would be too viscous, therefore this approach led to samples, which could be loaded.

2.2.2.3 SDS-PAGE

2.2.2.3.1 Mini-PROTEAN® Tetra Vertical Electrophoresis Cell

For separation of proteins according to their mass a discontinuous SDS-polyacrylamide gel was used. The stacking gel contained 4 %, the separating gel 12 % polyacrylamide. First an electric current of 40 V was applied until the Bromphenolblue reached the border between stacking and separating gel, then the electric potential was increased to 100 V. When working with *N. magadii* proteins the electric potential was kept at 40 V to increase quality of separation. Gels were either stained with Coomassie or used for Western Blot.

2.2.2.3.2 PROTEAN® II XL Cell

For better separation results, the PROTEAN® II XL Cell was used. The stacking gel contained 4 % and the separating gel 10 % polyacrylamide. An electric current of 40 V was applied until the Bromphenolblue band reached the end of the gel.

2.2.2.4 Western Blot

After SDS-PAGE the gels were blotted on a nitrocellulose membrane with following settings: 25 V, 1 A, 30 minutes. Gels containing *N. magadii* crude extracts were incubated for five minutes in ddH_2O to remove excess salt, which could lead to poor blotting efficiency. Afterwards the membrane was incubated overnight at 4°C with 5 % milk powder in 1x TBS. All subsequent washing steps were done with 1x TBS. The membrane was washed three times for 10 minutes and incubated with the primary antibody for one hour at room temperature. Then again the membrane was washed three times for 10 minutes and the secondary antibody was applied for one hour. Finally the membrane was washed and developed using the SuperSignal® West Pico Chemiluminescent kit.

2.2.3 *E. coli* methods

2.2.3.1 Transformation of *E. coli*

Prior to transformation cells had to be made competent. To do so *E. coli* was inoculated to an OD_{600} of 0.1 in 100 ml of LB medium. At an OD_{600} of around 0.6 the cells were harvested by centrifugation with 6,000 g for 10 minutes at 4°C. The supernatant was discarded and the pellet resuspended in 40 ml MOPS I. The batch was incubated for 10 minutes on ice and again centrifuged (same setup as before). Again the supernatant was discarded and the pellet resuspended in 40 ml MOPS II. After incubation for 30 minutes on ice the cells were centrifuged one last time (same setup as before). The supernatant was

discarded, the pellet resuspended in 2 ml of MOPS IIa and split in 100 µl aliquots. Competent cells were stored at -80°C. One aliquot was used for transformation with one plasmid or one ligation batch. After adding DNA the cells were incubated on ice for 30 minutes. Subsequently the cells were incubated at 42°C for two minutes and then on ice for 30 seconds. 300 µl of LB were added and cells were placed for regeneration on 37°C for 30 minutes without shaking. Three times 100 µl of cell suspension were plated on selective medium. Colonies were inoculated in 5 ml of LB medium with antibiotics added for further investigation.

2.2.3.2 Quick prep

After transformation colonies were inoculated in 5 ml of LB with the selective antibiotics, in order to test for positive clones. The cells were incubated overnight on 37°C while shaking. 300 µl of the overnight culture were centrifuged with 20,000 g for three minutes on room temperature. The supernatant was removed and the pellet was resuspended in 30 µl of 6x DNA loading dye. Afterwards 14 µl of phenol/chloroform (1:1) was added to the cell suspension and the cells were vortexed for 30 seconds following a centrifugation for five minutes with 20,000 g on room temperature. 12 µl of the aqueous phase was loaded to a 0.8 % agarose gel. Putative positive clones were tested further with PCR or restriction digest.

2.2.4 *N. magadii* methods

2.2.4.1 Transformation of *N. magadii*

2, 4 and 6 ml of a fresh preculture were used to inoculate 60 ml of NVM^+ with bacitracin and grown on 37°C while shaking. At an OD_{600} of about 0.5-0.6 the culture was centrifuged with 5,500 g for 15 minutes at room temperature. The supernatant was discarded, the pellet

carefully resuspended in 30 ml of buffered high salt spheroplast solution with glycerol and proteinase K was added to a final concentration of 0.1 %. The cells were incubated at 42°C until at least 90 % of the cells were spheroplasts. The cells were distributed in 1.5 ml aliquots and used immediately or stored on -80°C to a maximum of one week.

One aliquot of competent cells was used for transformation. Therefore the cells were centrifuged with 10,000 rpm for three minutes at room temperature. The supernatant was discarded and the cells resuspended in 150 µl of buffered high salt spheroplast solution. 15 µl of 0.5 M EDTA were added and the cells incubated on room temperature for 10 minutes. 10 µl of DNA with a concentration of at least 300 ng/µl were added and incubated for five minutes on room temperature. Subsequently 150 µl of 60 % PEG-600 in unbuffered high salt spheroplast solution was added and the cells were incubated at room temperature for 30 minutes. After that, 1 ml of NVM^+ was added and then centrifuged with 10,000 rpm for five minutes at room temperature in order to wash the cells. The supernatant was discarded and 1 ml of fresh NVM^+ was added without resuspending the pellet. Again the cells were centrifuged and fresh NVM^+ was added. The cells were regenerated on 37°C while shaking until at least 90 % of the cells appeared as rods under the microscope. Finally the cells were plated on NVM^+ plates containing the selective antibiotics.

2.2.4.2 Measuring specific promoter strength using bgaH

Promoter strength was determined by using bgaH as a reporter gene. The assay was performed as described in Mike Dyall-Smith's Halohandbook Version 7.2.

2.2.5 Cloning strategies

2.2.5.1 Cloning of *bgaH* under the promoter of ORF43

The plasmid pRV1-pTna was isolated from *E. coli* and subsequently restricted with *Nde*I and *Bam*HI to obtain the *bgaH* gene. This fragment was ligated into pKS-p43 restricted with the same enzymes and *E .coli* XL-1 Blue was transformed with the resulting plasmid. For the Gibson Assembly® p43-bgaH was amplified by PCR using the *Phusion* Polymerase and the primers pKS-p43-BgaH_F/pKS-p43-BgaH_R. The plasmid pNB102 was restricted with *Xba*I to generate a linearized form and 3' overhangs. 30 fmol of insert were mixed with 8 fmol of vector DNA and incubated on 50°C for one hour. The whole batch was used for the transformation of *E. coli* XL-1 Blue. Subsequently *N. magadii* L13 were transformed with pNB102-p43-bgaH together with either pRo5-p43-ORF43 or empty pRo5.

2.2.5.2 pNB102-p34-ORF11

First, the sequence of ORF11 was amplified by PCR using the primers E-Kpn-2/ E-BgI-2 and restricted with *Bgl*II and *Kpn*I as well as the plasmid pKS-p34. The fragment was ligated into the plasmid and *E. coli* XL-1 Blue was transformed. This plasmid was restricted with *Kpn*I and *Xba*I to obtain the fragment p34-ORF11 which was ligated into pNB102.

2.2.5.3 pNB102-M-Eco-12

IN the beginning the 3' end of the sequence was amplified using the primers 36-3X and M-Eco-1 and restricted with *Xba*I and *Eco*RI. The fragment was ligated into pBlueScriptII KS (+) and *E. coli* XL-1 Blue was transformed with the ligation reaction. The fragment

obtained by PCR using the primers 34-Kpn and M-Eco-2 was inserted into this plasmid after restriction with *Eco*RI and *Kpn*I. Subsequently the fragment M-Eco-12 was acquired by restriction with *Xba*I and *Kpn*I and ligated into pNB102.

2.2.5.4 Production of antibodies against gp22

During the first attempt the whole ORF22 was cloned into pQE30 and expressed. Therefore ORF22 was amplified by PCR with primers 22-Bam and 22-Bgl and ligated into pQE30 and pRSET-A. The resulting plasmid was used for transformation of *E. coli* strains Tuner and Rosetta. However it was impossible to purify the protein. So the protein was split into two parts and the 5'-end of the gene consisting 274 out of 452 codons was cloned into pQE30 and pRSET-A. For the PCR primers 22-Bam and 22-N-Hind were used. *E. coli* strains Tuner, Rosetta and BL-21 were chosen for expression studies.

3 Results and Discussion

3.1 Investigation of the putative regulatory function of gp43

Genetic (IRO *et al.*, 2007) as well as first biochemical data (HOFBAUER, 2015; LEBHARD, 2016) led to the assumption that the operon ORF43/44 could encode a TA-system. As mentioned before, due to the Pfam analysis, ORF43/44 should belong to the type II TA-systems. Here, the antitoxin regulates its own expression by interfering with its own promoter (MASUDA & INOUYE, 2017). Therefore, gp43, the putative antitoxin, could repress its own expression.

3.1.1 Experimental setup

To investigate this matter the reporter gene *bgaH* was used. According to 2.2.5.1 "Cloning of *bgaH* under the promoter of ORF43" the gene was cloned under the promoter of the operon ORF43/44. *N. magadii* L13 was transformed with two plasmids: pNB102-p43-bgaH and pRo-5-p43-ORF43. *N. magadii* L13 (pNB102-p43-bgaH/pRo-5) was used as a

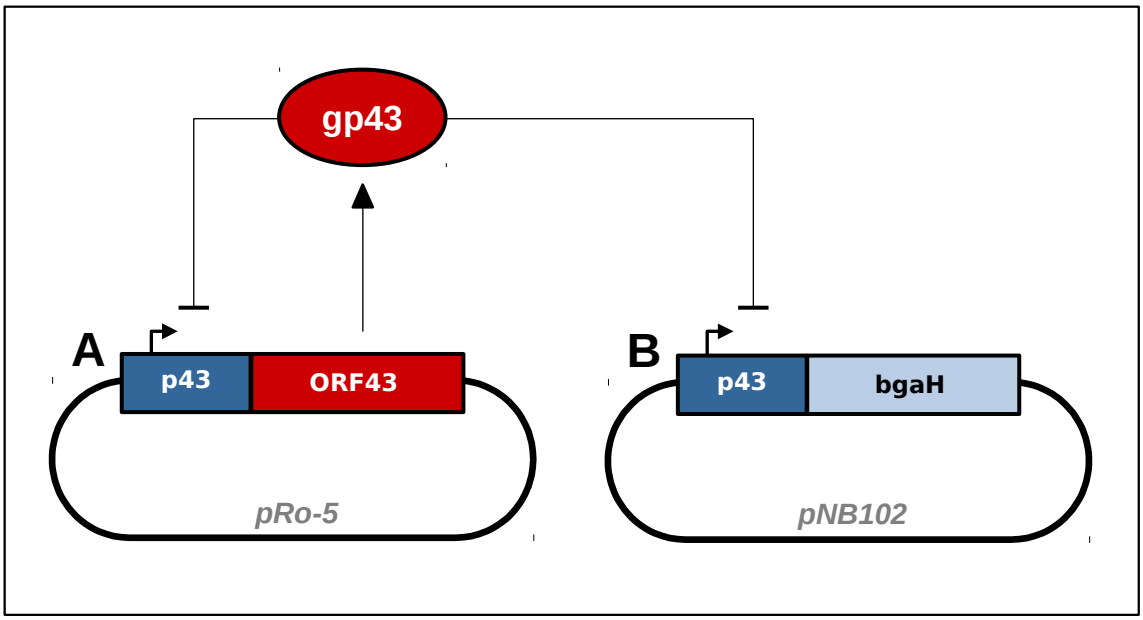

Figure 11: Hypothesized mode of action of gp43. As the putative antitoxin, gp43 could repress the promoter of the operon ORF43/44.

control . The hypothesized mode of action of gp43 can be seen in Figure 11. The putative antitoxin gp43 could have an autoregulatory function like other antitoxins of type-II TA-systems. So the presence of gp43 should repress the expression of the *bgaH* gene, therefore the specific β-galactosidase activity should be lower than that of the control.

The cultures were inoculated to an OD_{600} of 0.1 and grown at 37°C while shaking. The following three days the cell density was measured (OD_{600}) and samples were taken. Therefore, 1.5 ml of the culture were centrifuged and the pellets were resuspended in 375 µl 2 M NaCl solution. The cell suspension was stored at -20°C until all samples were taken. The last sample was kept on -20°C overnight to provide equal treatment of all samples. From now on the protocol by Mike Dyall-Smith's Halohandbook Version 7.2 chapter 6.5.3 was followed. Absorption at 405 nm was measured directly after addition of ONPG as well 2, 5 and 10 minutes afterwards.

3.1.2 Results

First, the growth kinetics of both strains were compared (see Figure 12 A&B). Both strains grew almost identically, therefore different expression levels of *bgaH* are not biased by different growth of these strains. As mentioned above, a sample was taken each day and each sample was measured 5 times. In Figure 12 C the specific BgaH activity on all three days can be seen. While on day two and three both strains show almost the same activity, day one shows a significant difference. Here, higher BgaH activities could be measured for strain *N. magadii* L13 (pNB102-p43-bgaH/pRo-5-p43-ORF43) than for the control strain. However, in contrast to what was hypothesized, the activity in the strain with the putative repressor showed almost twice as much activity compared to the control.

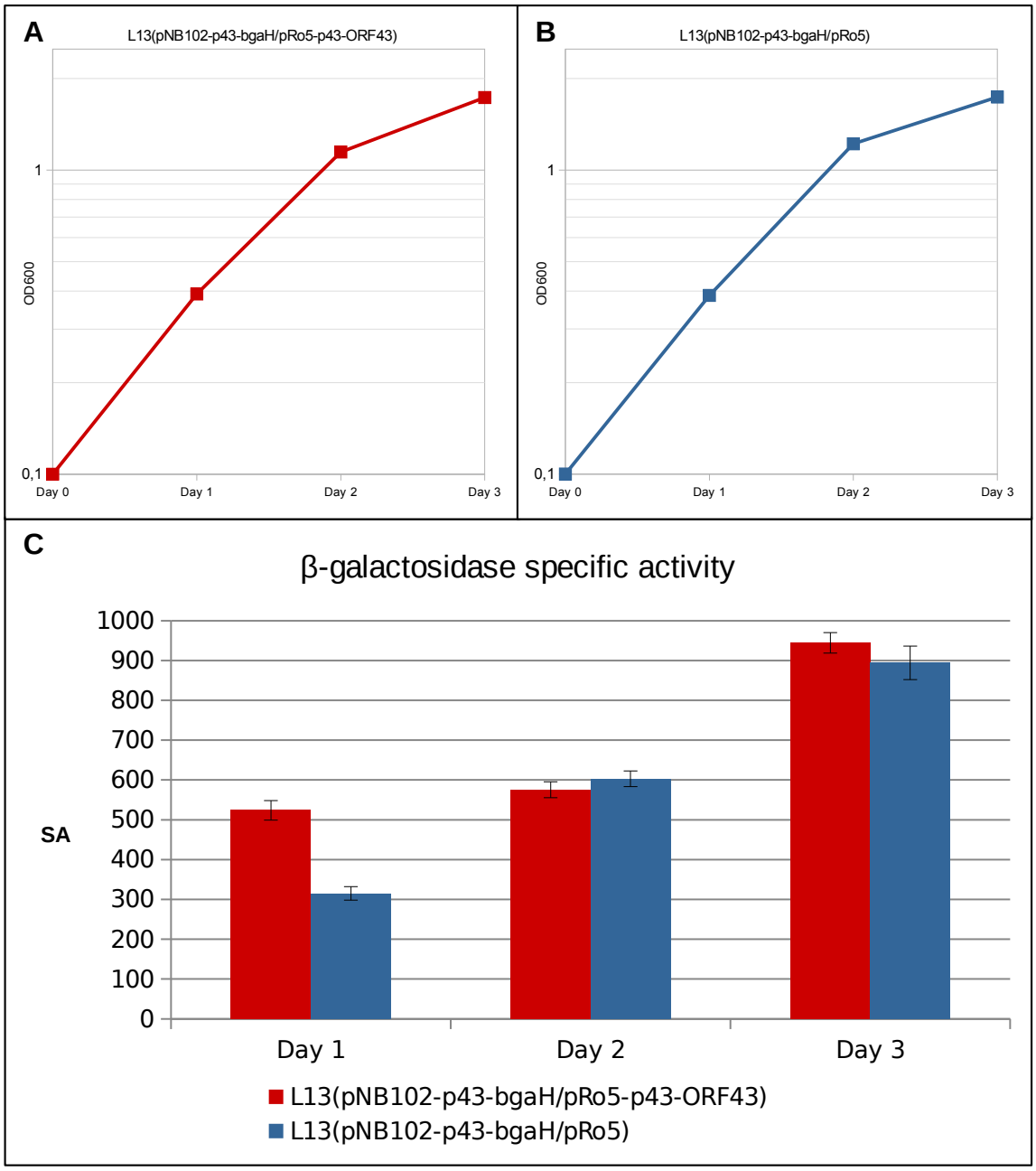

Figure 12: Growth curves and specific β-galactosidase acitvity of *N. magadii* L13 (pNB102-p43-bgaH/pRo-5-p43-ORF43) and *N. magadii* L13 (pNB102-p43-bgaH/pRo-5). In A&B the growth curves are shown. Both strains grew almost identical over the three day period. C shows the specific β-galactosidase activity of both strains. In red *N. magadii* L13 (pNB102-p43-bgaH/pRo-5-p43-ORF43) and in blue *N. magadii* L13 (pNB102-p43-bgaH/pRo-5) are compared. Only Day 1 shows a significant difference in activity.

3.1.3 Discussion

Figure 12 C shows the expression levels of *bgaH*. A reason for the high basal level of *bgaH* activity could lie in the construct pRo-5-p43-ORF43. Since the putative antitoxin should be able to repress its own promoter, it is possible that most of the repressors are

“stuck” on the promoter on the plasmid pRo-5 and therefore are not able to repress expression of *bgaH*. Additionally, the copy number of the plasmids can also be a reason for the high expression level. Since pNB102 is a high copy plasmid and pRo-5 is a low copy plasmid, the above mentioned effect is enhanced, so that the strain *N. magadii* L13 (pNB102-p43-*bgaH*/pRo-5-p43-ORF43) has the same β-galactosidase activity as an unrepressed strain.

3.1.4 Future outlook

This experimental setup represents the preliminary investigation of the interaction between gp43 and the promoter sequence of the operon ORF43/44. To get a clear picture of the situation, ORF43 should be cloned under a constitutive promoter like p34 of ΦCh1 ORF34 (SELB *et al*., 2017) or an inducible one like ptnaN of *N. magadii* (ALTE, 2011). It is reported that in some TA-systems the TA-complex has stronger binding affinity to the promoter sequence than the antitoxin alone (GOTFREDSEN & GERDES, 1998). This applies especially true for TA-systems which belong to the VapBC family. Therefore, this aspect should be investigated too by putting the operon ORF43/44 under an inducible promoter. By comparing the results of these two experiments, sharp conclusions can be drawn, whether the operon ORF43/44 autoregulates itself by binding of gp43 or the complex gp43/44.

3.2 Characterization of gp22

As mentioned before (see 1.2.2.3 "The operon ORF43/44"), the sequence of ORF22 contains a putative target sequence for gp44, this ORF22 was investigated in more detail. Beside the verification as a target for gp44, the function of the encoded protein was investigated. The localization of ORF22 within a cluster of genes responsible for the assembly and morphology (KLEIN *et al*., 2002), it was assumed that gp22 is capsid protein. Therefore, the gene was cloned and expressed in *E. coli*. A fresh overnight culture of *E. coli* XL-1 Blue (pQE-30-ORF22) was inoculated to an OD_{600} of 0.1 and grown to an OD_{600} of 0.3. The culture was induced with IPTG and was agitated at 37°C for 2 hours. A crude extract sample for Western Blot analysis with α-His and α-ΦCh1 was taken. The results ca be seen in Figure 13.

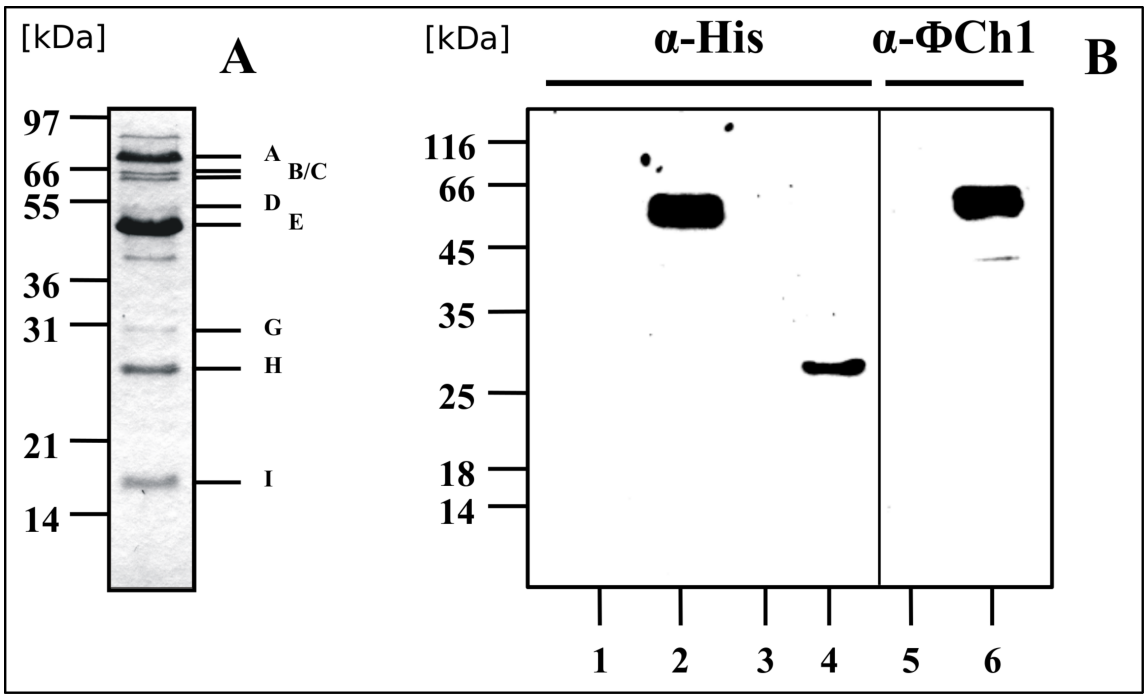

Figure 13: Expression of gp22 in *E.* coli. A shows the protein pattern of ΦCh1 particles which were precipitated with TCA and separated with a SDS-PAGE. Protein bands were designated as reported by Witte *et al.* in 1997. Adapted from Klein *et al.*, 2002. B shows two different Western Blots. Lane 1: *E. coli* XL-1 Blue(pQE30-ORF22) before induction with IPTG, lane 2: *E. coli* XL-1 Blue(pQE30-ORF22) two hours after induction with IPTG, lane 3: *E. coli* XL-1 Blue(pQE30) two hours after induction with IPTG, lane 4: 6xHis-tagged ORF19 as a positive control, lane 5: *E. coli* XL-1 Blue(pQE30-ORF22) before induction with IPTG, lane 6: *E. coli* XL-1 Blue(pQE30-ORF22) two hours after induction with IPTG. In lane 1-4 α-His and in lane 5 and 6 α-ΦCh1 antibodies were used for detection.

The approximately 48 kDa heavy protein was detectable by α-His as well as α-ΦCh1 antibodies (see Figure 13B). This data supports the hypothesis that ORF22 is encoding for a capsid protein.

3.2.1 Production of antibodies against gp22

In order to investigate expression of ORF22 on protein level, production of antibodies against gp22 is necessary. This was achieved by purifying the N-terminal part of gp22 from *E. coli* and subsequently generation of polyclonal antibodies.

The first expression to purify gp22 was done in *E. coli* strains Tuner and Rosetta with pQE30-ORF22 and pRSET-A-ORF22. However, it was impossible to isolate protein. After Western blot analysis with antibodies against a 6xHis-Tag showed no signal, so gp22 was tagged at the C-terminal part by cloning ORF22 into pQE16. The *E. coli* strains BL21, Tuner and Rosetta were transformed with the plasmid pQE16-ORF22. Unfortunately, the isolation of the protein failed again, despite of trying different protocols and purification conditions. Therefore, ORF22 was split into two parts. The N-terminal part of the protein

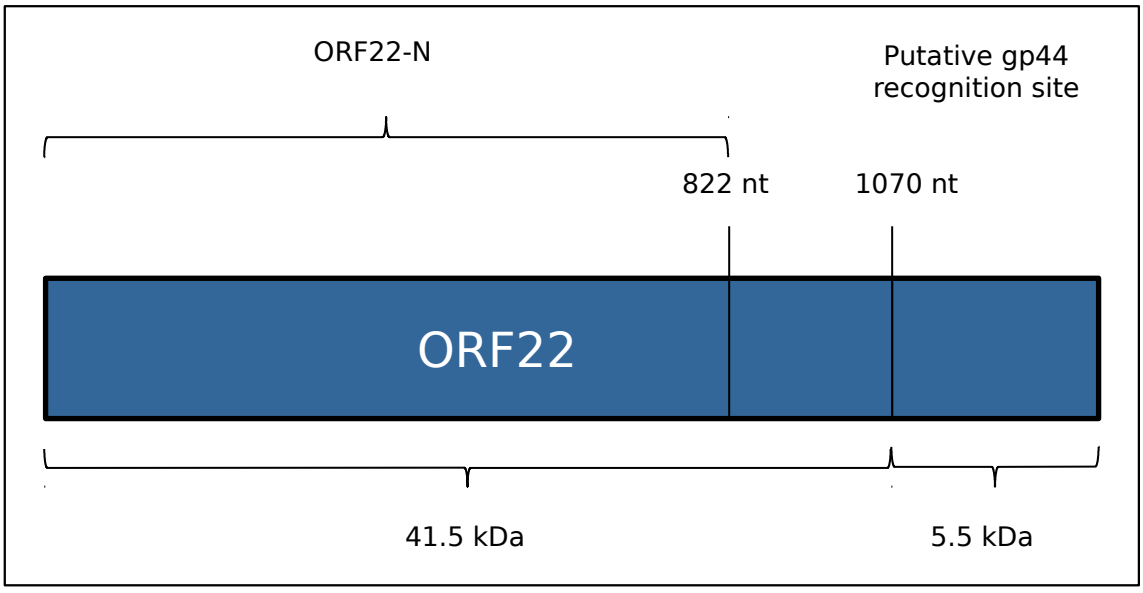

Figure 14: Schematic drawing of ORF22. Marks indicate where ORF22 was split for the generation of ORF22-N and the putative recogintion site of gp44.

was chosen, since it is the larger part of the protein (see Figure 14). The resulting ORF22-N was cloned into pQE30 and pRSET-A. Again the *E. coli* strains BL21, Tuner and Rosetta were transformed and a test-expression was performed. The cultures were inoculated to an OD_{600} of 0.1 and grown at 37°C while shaking. At an optical density of about 0.3 the cultures were induced with IPTG and samples were taken every 30 minutes for Western blot analysis with α-His and α-ΦCh1 antibodies.

As expression of *E. coli* Tuner(pRSET-A-ORF22-N) was best, which was determined by Western Blot analysis, this strain was chosen to isolate gp22-N. This was done according to the protocol 2.2.2.1 "Purification of His-tagged protein from *E. coli*". The purified protein was sent to the company "Moravian-Biotechnology Ltd." for immunization of rabbits. The resulting sera were thoroughly tested for specificity and sensitivity.

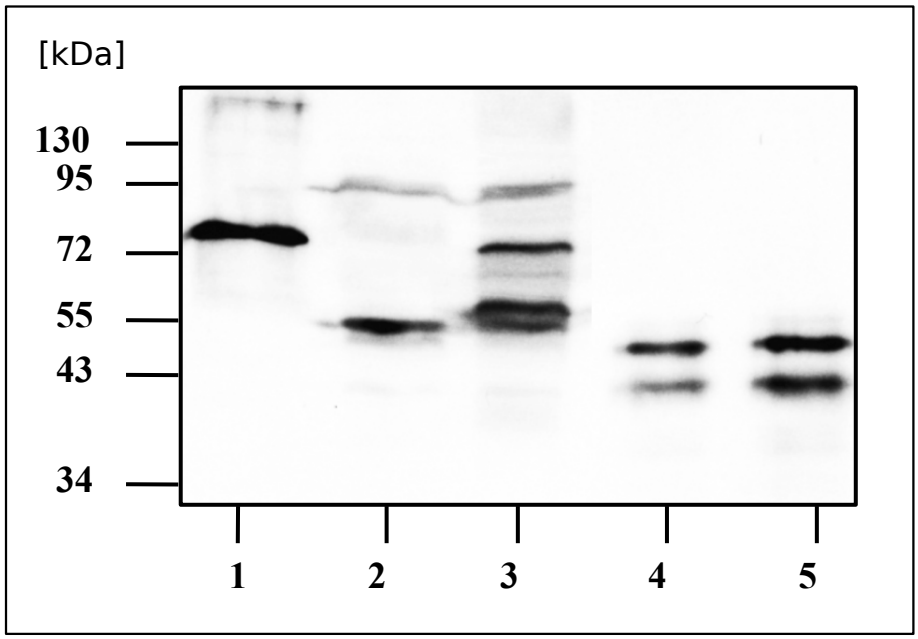

Figure 15: Western Blot of the last serum received from Moravian-Biotechnology. Lane 1: ΦCh1 virus particles, lane 2: *N. magadii* L13, lane 3: *N. magadii* L11, lane 4: purified gp22-N (1:50), lane 5: gp22-N (1:25). There are unspecific bands, however there is specific band in lane 1 as well as in lane 3 indicating that the antibodies can detect gp22.

As shown in Figure 15, the serum can detect gp22 as well as gp22-N. However, the Western Blot analysis also displays unspecific recognition of other proteins. Nonetheless, the antibodies can be used for further investigations involving ORF22 in *N. magadii*, if a proper control is loaded in addition on the same SDS-gel.

3.2.2 Expression of gp22 in *N. magadii* L11

First, the expression of ORF22 was followed during the growth of *N. magadii* L11. The strain was inoculated to an OD_{600} of 0.1 and incubated at 37°C while shaking. Crude extract protein samples were taken each day and analyzed by Western Blot.

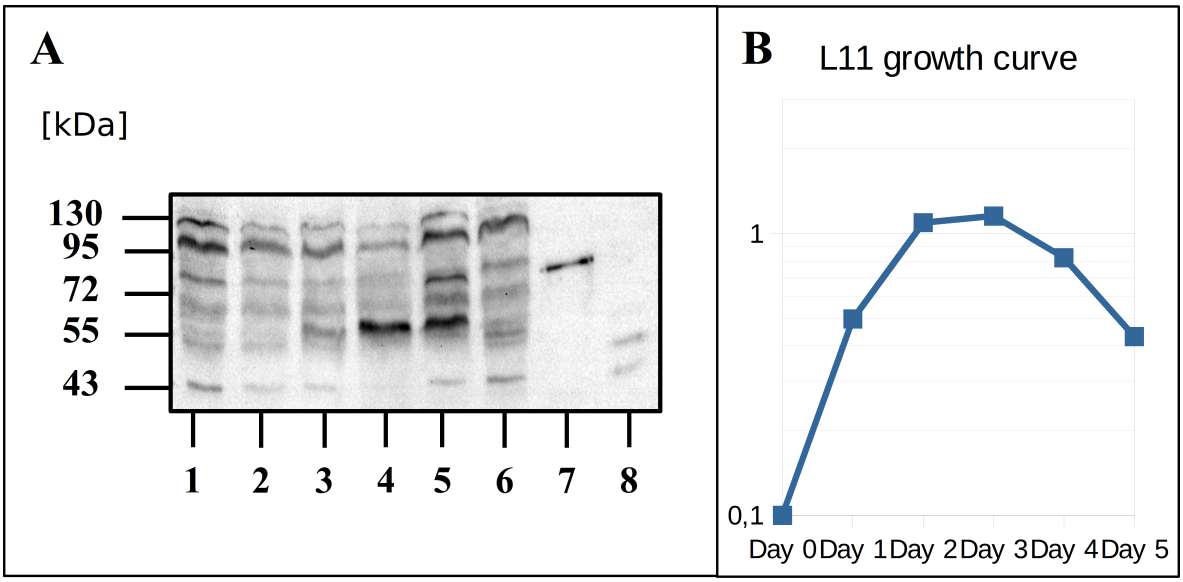

Figure 16: Time kinetics of ORF22 in *N. magadii* L11. A shows the Western Blot of the time series of 5 days. Lane 1: *N. magadii* L13; lane 2-6: *N. magadii* L11 day 1-5; lane 7: ΦCh1 virus particles; lane 8: gp22-N positive control.

3.2.3 Identification of new putative targets of gp44

Since gp44 could have a PIN-domain and an effect on $gp34_{52}$ and Mtase can be seen (HOFBAUER, 2015; LEBHARD, 2016), new putative targets were identified by sequence analysis (see Figure 8). ORF11, the major capsid protein, and ORF22, the minor capsid protein of ΦCh1, were chosen to be investigated in regards of being targets of gp44 too.

3.2.3.1 Experimental setup

The genes ORF11 and ORF22 were cloned into the plasmid pNB102 under the constitutive promoter p34 (SELB *et al*., 2017). *N. magadii* L13 was transformed with these plasmids together with the plasmid pRo-5-ptnaN-ORF44 (see Figure 17). The promoter of ptnaN of *N. magadii* is inducible with tryptophan (SCHÖNER, 2013), so expression of the putative toxin can be induced by addition of tryptophan. First, a preculture in $NMMb^+$ was produced to remove the tryptophan which is present in NVM^+. Subsequently, the cultures

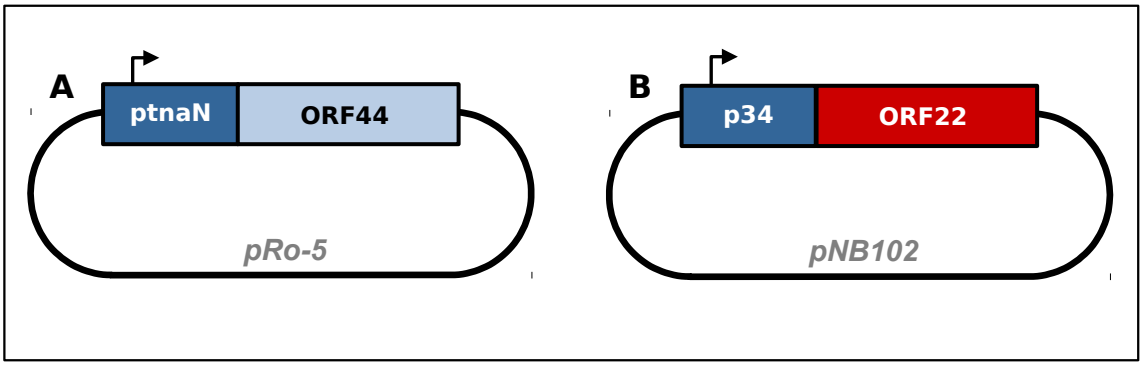

Figure 17: Plasmids used for investigation if ORF22 is a target of gp44. ORF44 is under the inducible promoter ptnaN (A) and ORF22 under the constitutive promoter p34 (B)

were inoculated in $NMMb^+$ to an OD_{700} of 0.1 and grown on 37°C while shaking. Since *N. magadii* has a chromosomally encoded tryptohanase, the inducer had to be added daily. As soon as the culture reached an OD_{700} of 0.3, the first sample was taken and then tryptophan was added to the culture. Each day the optical density was measured, a sample taken and new tryptophan added. The samples were prepared for Western Blot analysis according to 2.2.2.2.2 "Crude extract protein samples from *N. magadii*" and separated on a 10% polyacrylamide gel using the Bio-Rad PROTEAN® II XL Cell.

3.2.3.2 Results

Unfortunately, it was impossible to find a positive clone of *N. magadii* L13 (pNB102-p34-ORF11/pRo-5-ptnaN-ORF44) which expresses ORF11 within the given time. However, an expressing strain of *N. magadii* L13 (pNB102-p34-ORF22/pRo-5-ptnaN-ORF44) was isolated. The Western blot analysis of the timecourse experiment is shown in Figure 18. On the eighth day of induction with 2 mM tryptophan, a second band below the gp22 band appears. In Figure 14 the schematic drawing of ORF22 is shown where the putative recognition site of gp44 is marked. If gp44 has RNase activity on the transcript of ORF22, the truncated protein should be approximately 5.5 kDa smaller. This fits exactly what can be observed by Western blot analysis.

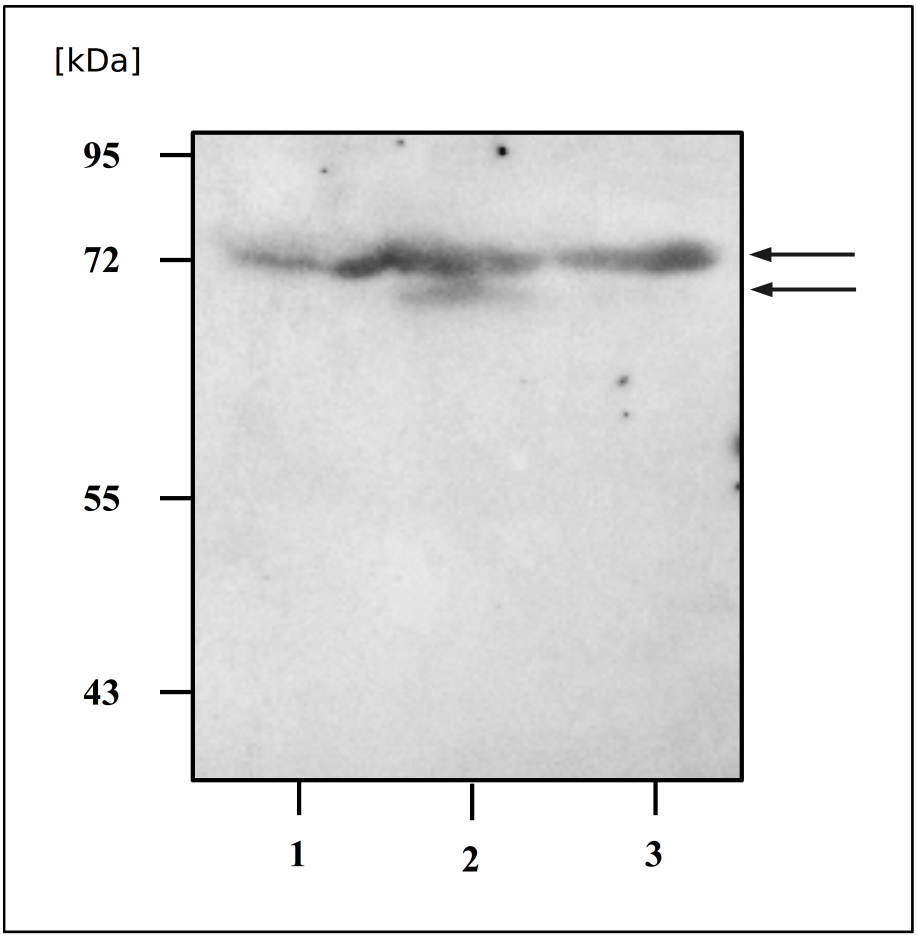

Figure 18: Western blot of *N. magadii* L13(pNB102-p34-ORF22/pRo-5-ptnaN-ORF44) time series. Lane 1: before induction with tryptophan, lane 2: 9th day after induction, lane 3: *N. magadii* L13.

3.2.3.3 Discussion

Since this was a preliminary experiment to prove the activity of gp44. It was unknown whether this setup would work or not. However, in lane 10 the appearance of a new band is found. The activity of gp44, resulting in a truncated version of gp22 is shown in Figure 18. The expected truncation of gp22 can be seen. The full-length protein has a molecular weight of about 47 kDa. The putative truncated protein has 41.5 kDa. The discrepancy between its actual size and the observed size can be explained by the isoelectric point of gp22 at a pH of 4.06. Due to this low isoelectric point gp22 migrates through the gel slower and therefore seems to have a larger size.

3.2.3.4 Future outlook

This experiment needs to be repeated with a larger volume of culture in order to take samples over a longer period of time. It is highly possible that the additional signal which can be seen in lane 10 will become stronger. Together with a proper control, it can be investigated, whether gp44 has a direct influence on the expression of ORF22 or not. To see if really gp44 is responsible for the additional band, the way to choose should be to split the culture before induction with tryptophan. The uninduced part of the culture serves as a negative control to eliminate background activity of gp44. Additionally a second strain *N. magadii* L13 (pNB102-p34-ORF22/pRo-5) can be used as a negative control. With these two ways it is possible to verify that induction of gp44 is the actual trigger for the appearance of the additional band.

4 Résumé

Not all aims of this thesis were reached within the given time. It could be shown that gp44 has an impact on the expression of ORF22. The appearance of a truncated gp22 of about the expected size from the putative recognition is a promising result for future experiments. This experiment needs to be repeated, in order to confirm that the induction of ORF44 is responsible for the phenotype observed. Furthermore, the sensitivity of α-gp22-N antibodies was shown in an experiment.

The next steps to further characterize gp44 include purification of the protein under native conditions for in-vitro experiments. These experiments should determine, if gp44 has actual RNase activity and whether this activity is sequence-specific or not. If gp44 is a sequence-specific RNase, the targets in the *N. magadii* and especially in the ΦCh1 genome are of great interest. Subsequently, the role of gp43 needs to be investigated. Is gp43 able to neutralize the activity of gp44? Does gp43 or the complex of gp43/44 repress the expression of ORF43/44? All this information would support the hypothesis, that the operon ORF43/44 is a VapBC-like TA-system.

5 References

AIZENMAN, E., ENGELBERG-KULKA, H., & GLASER, G. (1996): An Escherichia coli chromosomal "addiction module" regulated by guanosine [corrected] 3',5'-bispyrophosphate: a model for programmed bacterial cell death. *Proceedings of the National Academy of Sciences*, *93*, 6059–6063.

ALBERS, S.-V. V., & MEYER, B. H. (2011): The archaeal cell envelope. *Nature Reviews Microbiology*, *9*, 414–426.

ALTE, B. (2011): Konstruktion einer Flagellum-Deletionsmutante in Natrialba magadii und Charakterisierung bestehender Natrialba magadii Mutanten ; diploma's thesis, University of Vienna.

ARCUS, V. L., MCKENZIE, J. L., ROBSON, J., & COOK, G. M. (2011): The PIN-domain ribonucleases and the prokaryotic VapBC toxin-antitoxin array. *Protein Engineering, Design and Selection*, *24*, 33–40.

ARNOLD, H. P., ZIESE, U., & ZILLIG, W. (2000): SNDV, a Novel Virus of the Extremely Thermophilic and Acidophilic Archaeon Sulfolobus. *Virology*, *272*, 409–416.

BARANYI, U., KLEIN, R., LUBITZ, W., KRÜGER, D. H., & WITTE, A. (2000): The archaeal halophilic virus-encoded Dam-like methyltransferase M.φCh1-I methylates adenine residues and complements dam mutants in the low salt environment of Escherichia coli. *Molecular Microbiology*, *35*, 1168–1179.

BAUMEISTER, W., WILDHABER, I., & PHIPPS, B. M. (1989): Principles of organization in eubacterial and archaebacterial surface proteins. *Canadian Journal of Microbiology*, *35*, 215–227.

BETTSTETTER, M., PENG, X., GARRETT, R. A., & PRANGISHVILI, D. (2003): AFV1, a novel virus infecting hyperthermophilic archaea of the genus Acidianus. *Virology*, *315*, 68–79.

BREITBART, M., WEGLEY, L., LEEDS, S., SCHOENFELD, T., & ROHWER, F. (2004): Phage Community Dynamics in Hot Springs. *Applied and Environmental Microbiology*, *70*, 1633–1640.

BROWN, B. L., GRIGORIU, S., KIM, Y., ARRUDA, J. M., DAVENPORT, A., WOOD, T. K., PETI, W., & PAGE, R. (2009): Three dimensional structure of the MqsR:MqsA complex: A novel TA pair comprised of a toxin homologous to RelE and an antitoxin with unique properties. *PLoS Pathogens*, *5*, e1000706.

BROWN, B. L., LORD, D. M., GRIGORIUS, S., PETI, W., & PAGES, R. (2013): The Escherichia coli toxin MqsR destabilizes the transcriptional repression complex

formed between the antitoxin MqsA and the mqsRA operon promoter. *Journal of Biological Chemistry*, *288*, 1286–1294.

CAVICCHIOLI, R. (2011): Archaea - Timeline of the third domain. *Nature Reviews Microbiology*, *9*, 51–61.

CHAN, W. T., ESPINOSA, M., & YEO, C. C. (2016): Keeping the Wolves at Bay: Antitoxins of Prokaryotic Type II Toxin-Antitoxin Systems. *Frontiers in Molecular Biosciences*, *3*, 1–20.

CHERNY, I., & GAZIT, E. (2004): The YefM antitoxin defines a family of natively unfolded proteins: Implications as a novel antibacterial target. *Journal of Biological Chemistry*, *279*, 8252–8261.

CLINE, S. W., & FORD DOOLITTLE, W. (1987): Efficient transfection of the archaebacterium Halobacterium halobium. *Journal of Bacteriology*, *169*, 1341–1344.

COOK, G. M., RUSSELL, J. B., REICHERT, A., & WIEGEL, J. (1996): The intracellular pH of Clostridium paradoxum, an anaerobic, alkaliphilic, and thermophilic bacterium. *Applied and Environmental Microbiology*, *62*, 4576–4579.

CRUZ, J. W., SHARP, J. D., HOFFER, E. D., MAEHIGASHI, T., VVEDENSKAYA, I. O., KONKIMALLA, A., HUSSON, R. N., NICKELS, B. E., DUNHAM, C. M., & WOYCHIK, N. A. (2015): Growth-regulating Mycobacterium tuberculosis VapC-mt4 toxin is an isoacceptor-specific tRNase. *Nature Communications*, *6*, 7480.

DANOVARO, R., DELL'ANNO, A., CORINALDESI, C., RASTELLI, E., CAVICCHIOLI, R., KRUPOVIC, M., NOBLE, R. T., NUNOURA, T., & PRANGISHVILI, D. (2016): Virus-mediated archaeal hecatomb in the deep seafloor. *Science Advances*, *2*, e1600492–e1600492.

DE JONGE, N., GARCIA-PINO, A., BUTS, L., HAESAERTS, S., CHARLIER, D., ZANGGER, K., WYNS, L., DE GREVE, H., & LORIS, R. (2009): Rejuvenation of CcdB-Poisoned Gyrase by an Intrinsically Disordered Protein Domain. *Molecular Cell*, *35*, 154–163.

DE JONGE, N., HOHLWEG, W., GARCIA-PINO, A., RESPONDEK, M., BUTS, L., HAESAERTS, S., LAH, J., ZANGGER, K., & LORIS, R. (2010): Structural and thermodynamic characterization of Vibrio fischeri CcdB. *Journal of Biological Chemistry*, *285*, 5606–5613.

DE ROSA, M., & GAMBACORTA, A. (1988): The lipids of archaebacteria. *Progress in Lipid Research*.

DIAGO-NAVARRO, E., HERNANDEZ-ARRIAGA, A. M., LÓPEZ-VILLAREJO, J., MUÑOZ-GÓMEZ, A. J., KAMPHUIS, M. B., BOELENS, R., LEMONNIER, M., & DÍAZ-OREJAS, R. (2010, August 1): ParD toxin-antitoxin system of plasmid R1 - Basic contributions,

biotechnological applications and relationships with closely-related toxin-antitoxin systems. *FEBS Journal*. Wiley/Blackwell (10.1111).

DÖRR, T., VULIĆ, M., & LEWIS, K. (2010): Ciprofloxacin causes persister formation by inducing the TisB toxin in Escherichia coli. *PLoS Biology*, *8*, e1000317.

DY, R. L., PRZYBILSKI, R., SEMEIJN, K., SALMOND, G. P. C., & FINERAN, P. C. (2014): A widespread bacteriophage abortive infection system functions through a Type IV toxin-antitoxin mechanism. *Nucleic Acids Research*, *42*, 4590–4605.

EDWARDS, M. A. (2018): "Stability of the ΦCh1 ORF44 deletion mutant and characterization of the function of gp44" ; masters thesis, University of Vienna.

EME, L., SPANG, A., LOMBARD, J., STAIRS, C. W., & ETTEMA, T. J. G. G. (2017): Archaea and the origin of eukaryotes. *Nature Reviews Microbiology*, *15*, 711–723.

FRANZMANN, P. D., LIU, Y., BALKWILL, D. L., ALDRICH, H. C., CONWAY DE MACARIO, E., & BOONE, D. R. (1997): Methanogenium frigidum sp. nov., a Psychrophilic, H2-Using Methanogen from Ace Lake, Antarctica. *International Journal of Systematic Bacteriology*, *47*, 1068–1072.

GARCIA-PINO, A., CHRISTENSEN-DALSGAARD, M., WYNS, L., YARMOLINSKY, M., MAGNUSON, R. D., GERDES, K., & LORIS, R. (2008): Doc of prophage P1 is inhibited by its antitoxin partner Phd through fold complementation. *Journal of Biological Chemistry*, *283*, 30821–30827.

GERDES, K., THISTED, T., & MARTINUSSEN, J. (1990): Mechanism of post-segregational killing by the hok/sok system of plasmid R1: sok antisense RNA regulates formation of a hok mRNA species correlated with killing of plasmid-free cells. *Molecular Microbiology*, *4*, 1807–1818.

GILLEN, Y. (2017): "Construction of mutant ΦCh1-ΔORF44, its characterization and first steps in the generation of mutant ΦCh1-ΔORF56" ; master's thesis, University of Vienna.

GOTFREDSEN, M., & GERDES, K. (1998): The Escherichia coli relBE genes belong to a new toxin-antitoxin gene family. *Molecular Microbiology*, *29*, 1065–1076.

GRANT, W. D. (2004): Life at low water activity. *Philosophical Transactions of the Royal Society B: Biological Sciences*, *359*, 1249–1267.

GUFFANTI, A. A., & HICKS, D. B. (1991): Molar growth yields and bioenergetic parameters of extremely alkaliphilic Bacillus species in batch cultures, and growth in a chemostat at pH 10.5. *Journal of General Microbiology*, *137*, 2375–2379.

GUY, L., & ETTEMA, T. J. G. (2011, December): The archaeal "TACK" superphylum and the origin of eukaryotes. *Trends in Microbiology*.

HAIDER, F. (2009): “Characterization of the DNA methyltransferase M .Nma Φ Ch1I and further characterization of a transformation system of haloalkaliphilic Archaea” ; diploma’s thesis, University of Vienna.

HAINES, T. H., & DENCHER, N. A. (2002, September 25): Cardiolipin: A proton trap for oxidative phosphorylation. *FEBS Letters*. No longer published by Elsevier.

HÄRING, M., RACHEL, R., PENG, X., GARRETT, R. A., & PRANGISHVILI, D. (2005): Viral Diversity in Hot Springs of Pozzuoli, Italy, and Characterization of a Unique Archaeal Virus, Acidianus Bottle-Shaped Virus, from a New Family, the Ampullaviridae. *Journal of Virology*, *79*, 9904–9911.

HÄRING, M., VESTERGAARD, G., RACHEL, R., CHEN, L., GARRETT, R. A., & PRANGISHVILI, D. (2005): Virology: Independent virus development outside a host. *Nature*, *436*, 1101–1102.

HARMS, A., BRODERSEN, D. E., MITARAI, N., & GERDES, K. (2018): Toxins, Targets, and Triggers: An Overview of Toxin-Antitoxin Biology. *Molecular Cell*, 1–17.

HARMS, A., MAISONNEUVE, E., & GERDES, K. (2016): Mechanisms of bacterial persistence during stress and antibiotic exposure. *Science*, *354*, aaf4268.

HOCHSTEIN, R. A., AMENABAR, M. J., MUNSON-MCGEE, J. H., BOYD, E. S., & YOUNG, M. J. (2016): Acidianus Tailed Spindle Virus: a New Archaeal Large Tailed Spindle Virus Discovered by Culture-Independent Methods. *Journal of Virology*, *90*, 3458–3468.

HOFBAUER, C. (2015): "The function of gp34 and its regulation by ORF79 of ϕ Ch1 as well as the influence of other regulation elements“ ; master’s thesis, Universtity of Vienna.

HUNTE, C., SCREPANTI, E., VENTURI, M., RIMON, A., PADAN, E., & MICHEL, H. (2005): Structure of a Na+/H+ antiporter and insights into mechanism of action and regulation by pH. *Nature*, *435*, 1197–1202.

IRO, M., KLEIN, R., GÁLOS, B., BARANYI, U., RÖSSLER, N., & WITTE, A. (2007): The lysogenic region of virus ϕCh1: Identification of a repressor-operator system and determination of its activity in halophilic Archaea. *Extremophiles*, *11*, 383–396.

ITO, M., GUFFANTI, A. A., ZEMSKY, J., IVEY, D. M., & KRULWICH, T. A. (1997): Role of the nhaC-encoded Na+/H+antiporter of alkaliphilic Bacillus firmus OF4. *Journal of Bacteriology*, *179*, 3851–3857.

KAMADA, K., & HANAOKA, F. (2005): Conformational change in the catalytic site of the ribonuclease YoeB toxin by YefM antitoxin. *Molecular Cell*, *19*, 497–509.

KAMEKURA, M., DYALL-SMITH, M. L., UPASANI, V., VENTOSA, A., & KATES, M. (1997): Diversity of alkaliphilic halobacteria: proposals for transfer of Natronobacterium vacuolatum, Natronobacterium magadii, and Natronobacterium pharaonis to

Halorubrum, Natrialba, and Natronomonas gen. nov., respectively, as Halorubrum vacuolatum comb. nov. *International Journal of Systematic Bacteriology*, *47*, 853–857.

KAMPHUIS, M. B., MONTI, M. C., VAN DEN HEUVEL, R. H. H., SANTOS-SIERRA, S., FOLKERS, G. E., LEMONNIER, M., DÍAZ-OREJAS, R., HECK, A. J. R., & BOELENS, R. (2007): Interactions between the toxin Kid of the bacterial parD system and the antitoxins Kis and MazE. *Proteins: Structure, Function and Genetics*, *67*, 219–231.

KAMPHUIS, M., CHIARA MONTI, M., H. VAN DEN HEUVEL, R., LOPEZ-VILLAREJO, J., DIAZ-OREJAS, R., & BOELENS, R. (2007): Structure and Function of Bacterial Kid-Kis and Related Toxin-Antitoxin Systems. *Protein & Peptide Letters*, *14*, 113–124.

KASARI, V., KURG, K., MARGUS, T., TENSON, T., & KALDALU, N. (2010): The Escherichia coli mqsR and ygiT genes encode a new toxin-antitoxin pair. *Journal of Bacteriology*, *192*, 2908–2919.

KITADA, M., HASHIMOTO, M., KUDO, T., & HORIKOSHI, K. (1994): Properties of two different Na+/H+ antiport systems in alkaliphilic Bacillus sp. strain C-125. *Journal of Bacteriology*, *176*, 6464–9.

KLEIN, R., BARANYI, U., RÖSSLER, N., GREINEDER, B., SCHOLZ, H., & WITTE, A. (2002): Natrialba magadii virus φCh1: First complete nucleotide sequence and functional organization of a virus infecting a haloalkaliphilic archaeon. *Molecular Microbiology*, *45*, 851–863.

KLEIN, R., GREINEDER, B., BARANYI, U., & WITTE, A. (2000): The structural protein E of the archaeal virus ϕCh1: Evidence for processing in Natrialba magadii during virus maturation. *Virology*, *276*, 376–387.

KUMAR, P., ISSAC, B., DODSON, E. J., TURKENBURG, J. P., & MANDE, S. C. (2008): Crystal Structure of Mycobacterium tuberculosis YefM Antitoxin Reveals that it is Not an Intrinsically Unstructured Protein. *Journal of Molecular Biology*, *383*, 482–493.

LEBHARD, J. (2016): ORF43/44: A possible Toxin-Antitoxin system in ΦCh1 ; bachelor's thesis, FH Campus Wien.

LEVIN, I., SCHWARZENBACHER, R., PAGE, R., ABDUBEK, P., AMBING, E., BIORAC, T., BRINEN, L. S., CAMPBELL, J., CANAVES, J. M., CHIU, H. J., DAI, X., DEACON, A. M., DIDONATO, M., ELSLIGER, M. A., FLOYD, R., GODZIK, A., GRITTINI, C., GRZECHNIK, S. K., HAMPTON, E., JAROSZEWSKI, L., KARLAK, C., KLOCK, H. E., KOESEMA, E., KOVARIK, J. S., KREUSCH, A., KUHN, P., LESLEY, S. A., MCMULLAN, D., MCPHILLIPS, T. M., MILLER, M. D., MORSE, A., MOY, K., OUYANG, J., QUIJANO, K., REYES, R., REZEZADEH, F., ROBB, A., SIMS, E., SPRAGGON, G., STEVENS, R. C., VAN DEN BEDEM, H., VELASQUEZ, J., VINCENT, J., VON DELFT, F., WANG, X., WEST, B., WOLF, G., XU, Q., HODGSON, K. O., WOOLEY, J., & WILSON, I. A. (2004): Crystal

structure of a PIN (PilT N-terminus) domain (AF0591) from Archaeoglobus fulgidus at 1.90 Å resolution. *Proteins: Structure, Function and Genetics*, *56*, 404–408.

MADERN, D., PFISTER, C., & ZACCAI, G. (1995): Mutation at a Single Acidic Amino Acid Enhances the Halophilic Behaviour of Malate Dehydrogenase from Haloarcula Marismortui in Physiological Salts. *European Journal of Biochemistry*, *230*, 1088–1095.

MAKAROVA, K. S., GRISHIN, N. V., & KOONIN, E. V. (2006): The HicAB cassette, a putative novel, RNA-targeting toxin-antitoxin system in archaea and bacteria. *Bioinformatics*, *22*, 2581–2584.

MARTIN, A., YEATS, S., JANEKOVIC, D., REITER, W. D., AICHER, W., & ZILLIG, W. (1984): SAV 1, a temperate UV-inducible DNA virus-like particle from the archaebacterium Sulfolobus acidocaldarius isolate B12. *The EMBO Journal*, *3*, 2165–8.

MASUDA, H., & INOUYE, M. (2017, April 14): Toxins of prokaryotic toxin-antitoxin systems with sequence-specific endoribonuclease activity. *Toxins*. Multidisciplinary Digital Publishing Institute.

MAYRHOFER-IRO, M., LADURNER, A., MEISSNER, C., DERNTL, C., REITER, M., HAIDER, F., DIMMEL, K., RÖSSLER, N., KLEIN, R., BARANYI, U., SCHOLZ, H., & WITTEA, A. (2013): Utilization of virus φCh1 elements to establish a shuttle vector system for halo(alkali)philic Archaea via transformation of Natrialba magadii. *Applied and Environmental Microbiology*, *79*, 2741–2748.

MESBAH, N. M., COOK, G. M., & WIEGEL, J. (2009): The halophilic alkalithermophile Natranaerobius thermophilus adapts to multiple environmental extremes using a large repertoire of Na+(K+)/H+ antiporters. *Molecular Microbiology*, *74*, 270–281.

MOCHIZUKI, T., KRUPOVIC, M., PEHAU-ARNAUDET, G., SAKO, Y., FORTERRE, P., & PRANGISHVILI, D. (2012): Archaeal virus with exceptional virion architecture and the largest single-stranded DNA genome. *Proceedings of the National Academy of Sciences*, *109*, 13386–13391.

MONTI, M. C., HERNÁNDEZ-ARRIAGA, A. M., KAMPHUIS, M. B., LÓPEZ-VILLAREJO, J., HECK, A. J. R., BOELENS, R., DÍAZ-OREJAS, R., & VAN DEN HEUVEL, R. H. H. (2007): Interactions of Kid-Kis toxin-antitoxin complexes with the parD operator-promoter region of plasmid R1 are piloted by the Kis antitoxin and tuned by the stoichiometry of Kid-Kis oligomers. *Nucleic Acids Research*, *35*, 1737–1749.

OREN, A. (2012): The Function of Gas Vesicles in Halophilic Archaea and Bacteria: Theories and Experimental Evidence. *Life*, *3*, 1–20.

OREN, A., BRATBAK, G., & HELDAL, M. (1997): Occurrence of virus-like particles in the Dead Sea. *Extremophiles*, *1*, 143–149.

PEDERSEN, K., ZAVIALOV, A. V., PAVLOV, M. Y., ELF, J., GERDES, K., & EHRENBERG, M. (2003, January 10): The bacterial toxin RelE displays codon-specific cleavage of mRNAs in the ribosomal A site. *Cell*. Cell Press.

PETERS, J., NITSCH, M., KÜHLMORGEN, B., GOLBIK, R., LUPAS, A., KELLERMANN, J., ENGELHARDT, H., PFANDER, J. P., MÜLLER, S., GOLDIE, K., ENGEL, A., STETTER, K. O., & BAUMEISTER, W. (1995): Tetrabrachion: A Filamentous Archaebacterial Surface Protein Assembly of Unusual Structure and Extreme Stability. *Journal of Molecular Biology*, *245*, 385–401.

PRANGISHVILI, D., ARNOLD, H. P., GÖTZ, D., ZIESE, U., HOLZ, I., KRISTJANSSON, J. K., & ZILLIG, W. (1999): A novel virus family, the Rudiviridae: Structure, virus-host interactions and genome variability of the sulfolobus viruses SIRV1 and SIRV2. *Genetics*, *152*, 1387–1396.

PRANGISHVILI, D., BAMFORD, D. H., FORTERRE, P., IRANZO, J., KOONIN, E. V., & KRUPOVIC, M. (2017): The enigmatic archaeal virosphere. *Nature Reviews Microbiology*, *15*, 724–739.

REANNEY, D. C., & ACKERMANN, H. W. (1982): Comparative biology and evolution of bacteriophages. *Advances in Virus Research*, *27*, 205–280.

ROBSON, J., MCKENZIE, J. L., CURSONS, R., COOK, G. M., & ARCUS, V. L. (2009): The vapBC Operon from Mycobacterium smegmatis Is An Autoregulated Toxin-Antitoxin Module That Controls Growth via Inhibition of Translation. *Journal of Molecular Biology*, *390*, 353–367.

SCHLEPER, C., PUHLER, G., KUHLMORGEN, B., & ZILLIG, W. (1995, June 29): Life at Extremely Low pH. *Nature*. Nature Publishing Group.

SCHNABEL, H., ZILLIG, W., PFÄFFLE, M., SCHNABEL, R., MICHEL, H., & DELIUS, H. (1982): Halobacterium halobium phage ϕH. *The EMBO Journal*, *1*, 87–92.

SCHÖNER, L. (2013): Construction of different mutants of Natrialba magadii and the influence of different Ch1 ORFs on Natrialba magadii ; master's thesis, University of Vienna.

SELB, R., DERNTL, C., KLEIN, R., ALTE, B., HOFBAUER, C., KAUFMANN, M., BERAHA, J., SCHÖNER, L., & WITTE, A. (2017): The Viral Gene ORF79 Encodes a Repressor Regulating Induction of the Lytic Life Cycle in the Haloalkaliphilic Virus ϕCh1. *Journal of Virology*, *91*, e00206-17.

SOPPA, J. (1999, March 1): Normalized nucleotide frequencies allow the definition of archaeal promoter elements for different archaeal groups and reveal base-specific TFB contacts upstream of the TATA box [1]. *Molecular Microbiology*. Wiley/Blackwell (10.1111).

STURR, M. G., GUFFANTI, A. A., & KRULWICH, T. A. (1994): Growth and bioenergetics of alkaliphilic Bacillus firmus OF4 in continuous culture at high pH. *Journal of Bacteriology*, *176*, 3111–3116.

TAKAI, K., NAKAMURA, K., TOKI, T., TSUNOGAI, U., MIYAZAKI, M., MIYAZAKI, J., HIRAYAMA, H., NAKAGAWA, S., NUNOURA, T., & HORIKOSHI, K. (2008): Cell proliferation at 122 C and isotopically heavy CH4 production by a hyperthermophilic methanogen under high-pressure cultivation. *Proceedings of the National Academy of Sciences*, *105*, 10949–10954.

TENCHOV, B., VESCIO, E. M., SPROTT, G. D., ZEIDEL, M. L., & MATHAI, J. C. (2006): Salt tolerance of archaeal extremely halophilic lipid membranes. *The Journal of Biological Chemistry*, *281*, 10016–23.

TINDALL, B. J., ROSS, H. N. M., & GRANT, W. D. (1984): Natronobacterium gen. nov. and Natronococcus gen. nov., Two New Genera of Haloalkaliphilic Archaebacteria. *Systematic and Applied Microbiology*, *5*, 41–57.

TORSVIK, T., & DUNDAS, I. D. (1974): Bacteriophage of Halobacterium salinarium. *Nature*, *248*, 680–681.

WANG, X., LORD, D. M., CHENG, H. Y., OSBOURNE, D. O., HONG, S. H., SANCHEZ-TORRES, V., QUIROGA, C., ZHENG, K., HERRMANN, T., PETI, W., BENEDIK, M. J., PAGE, R., & WOOD, T. K. (2012): A new type V toxin-antitoxin system where mRNA for toxin GhoT is cleaved by antitoxin GhoS. *Nature Chemical Biology*, *8*, 855–861.

WINTHER, K. S., & GERDES, K. (2009): Ectopic production of VapCs from Enterobacteria inhibits translation and trans-activates YoeB mRNA interferase. *Molecular Microbiology*, *72*, 918–930.

WITTE, A., BARANYI, U., KLEIN, R., SULZNER, M., LUO, C., WANNER, G., KRÜGER, D. H., & LUBITZ, W. (1997): Characterization of Natronobacterium magadii phage phi Ch1, a unique archaeal phage containing DNA and RNA. *Mol. Microbiology Microbiology*, *23*, 603–616.

WOESE, C. R., & FOX, G. E. (1977): Phylogenetic structure of the prokaryotic domain: The primary kingdoms. *Proceedings of the National Academy of Sciences*, *74*, 5088–5090.

WOESE, C. R., KANDLER, O., & WHEELIS, M. L. (1990): Towards a natural system of organisms: proposal for the domains Archaea, Bacteria, and Eucarya. *Proceedings of the National Academy of Sciences of the United States of America*, *87*, 4576–9.

WOMMACK, K. E., & COLWELL, R. R. (2000): Virioplankton: Viruses in Aquatic Ecosystems. *Microbiology and Molecular Biology Reviews*, *64*, 69–114.

YAMAGUCHI, Y., NARIYA, H., PARK, J. H., & INOUYE, M. (2012): Inhibition of specific gene expressions by protein-mediated mRNA interference. *Nature Communications*, *3*, 607.

YAMAGUCHI, Y., PARK, J.-H., & INOUYE, M. (2011): Toxin-antitoxin systems in bacteria and archaea. *Annual Review of Genetics*, *45*, 61–79.

YAMAGUCHI, Y., PARK, J. H., & INOUYE, M. (2009): MqsR, a crucial regulator for quorum sensing and biofilm formation, is a GCU-specific mRNA interferase in Escherichia coli. *Journal of Biological Chemistry*, *284*, 28746–28753.

ZHANG, Y., & INOUYE, M. (2009): The inhibitory mechanism of protein synthesis by YoeB, an escherichia coli toxin. *Journal of Biological Chemistry*, *284*, 6627–6638.

ZHOU, M., XIANG, H., SUN, C., & TAN, H. (2004): Construction of a novel shuttle vector based on an RCR-plasmid from a haloalkaliphilic archaeon and transformation into other haloarchaea. *Biotechnology Letters*, *26*, 1107–1113.

List of Figures

Zusammenfassung

Der temperente Virus ΦCh1 infiziert das haloalkaliphile Archeon *Natrialba magadii*. Eine Untersuchung des offenen Leserahmens 44 (ORF44) zeigte in der Pfam Datenbank, dass ORF44 eine „PilT N terminal domain" (PIN-Domäne) enthält. Dieser bildet zusammen mit ORF43 ein Operon, da sie co-transkripiert und co-translatiert wird. Das führte zu der Hypothese, dass es sich bei ORF43/44 um ein Toxin-Antitoxin System (TA-System) handelt, das zu der VapBC Familie der Typ II TA-Systeme. Das VapBC TA-System besteht aus dem stabilen Toxin VapC das RNase Aktivität auf Grund der PIN-Domäne hat und dem labilen Antitoxin VapB, welches in der Lage ist die Toxizität zu neutralisieren. Diese TA-Operons werden entweder von dem Antitoxin oder dem TA-Komplex autoreguliert.

Voran gegangene Untersuchungen zeigten, dass das Genprodukt (gp44) einen Einfluss auf die Expression von $ORF34_{52}$, welcher das „tailfibre" Protein des Virus codiert und ORF94, welcher für eine Methyltransferase codiert, hat. Um ORF44 besser charakterisieren zu können, wurde ein neues Protein identifiziert, auf dessen Expression gp44 Einfluss haben könnte: ORF22. Es wurde gezeigt, dass gp22 Bestandteil des Viruscapsids von ΦCh1 ist und dass Expression von ORF44 zu einer verkürzten Version von gp22. Diese Daten unterstützen die Hypothese, dass es sich bei gp44 um eine RNase handelt.

Zusätzlich wurde die autoregulatorische Funktion von ORF43 untersucht. Dieses Experiment sollte in einer virusfreien Umgebung ablaufen, jedoch war die Negativkontrolle für dieses Experiment mit ΦCh1 infiziert. Trotzdem konnte gezeigt werden, dass der Promoter des Operons ORF43/44 ein konstitutiver ist.